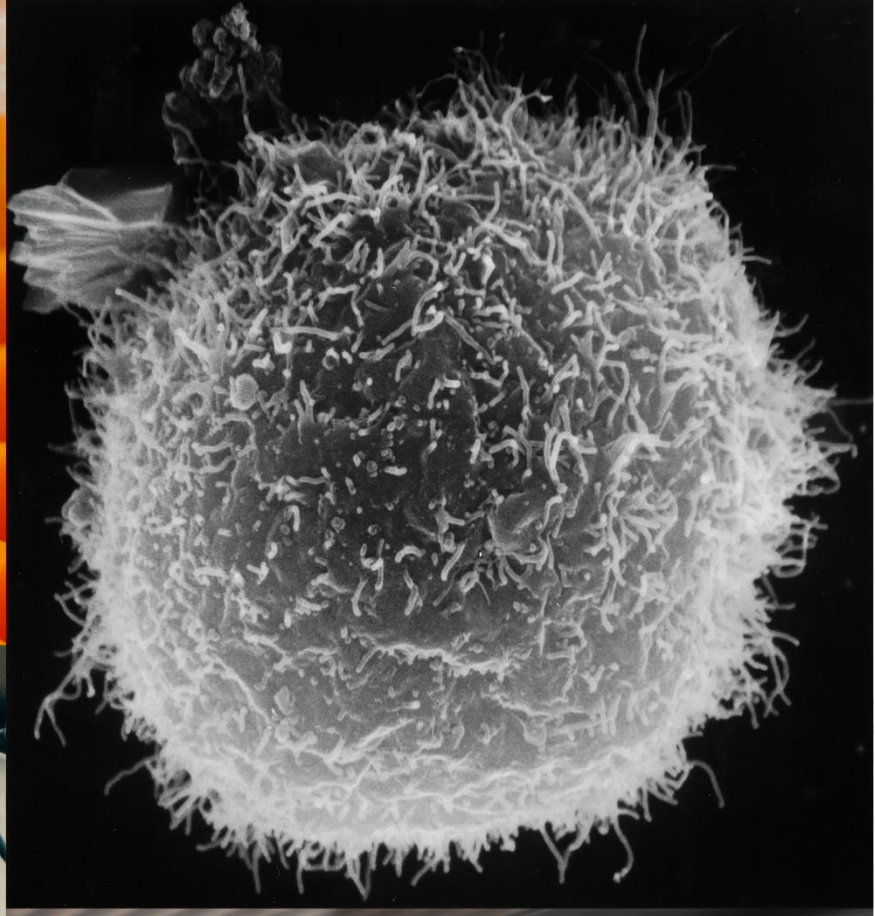

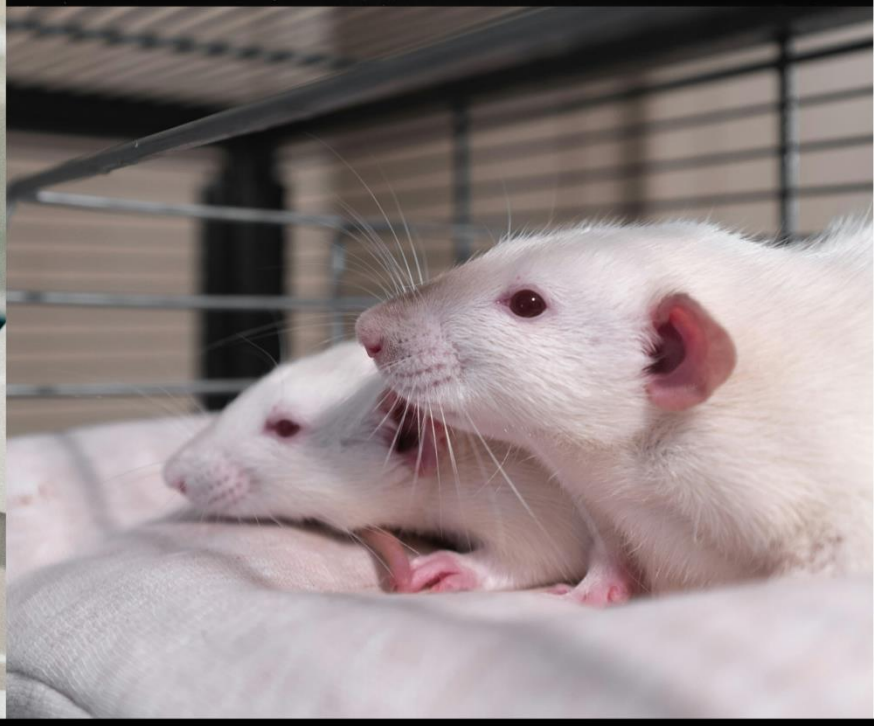

2022-24

BSURP

The BioScientific Undergraduate Research Publication

BSA BIOLOGY STUDENTS' ASSOCIATION

Table of Contents

What is BSURP?

The BioScientific Undergraduate Research Publication (BSURP) is a collection of summaries detailing research projects that were undertaken by Biological Sciences undergraduate students at the University of Calgary. As one of the top research universities in Canada, the University of Calgary provides many students with incredible opportunities to conduct innovative research in many diverse areas. Many students in the Biological Sciences have taken up research as part of summer programs or as courses for their degree.

The Biology Students' Association (BSA) began the BSURP during the 2020-21 academic year in order to highlight the amazing research being done by our fellow Biological Sciences students. Students from diverse backgrounds, both academic and non-academic, have been proudly represented in the publication. Projects were conducted in research labs both within and outside the Biological Sciences department, covering a diverse range of interesting and ground-breaking topics.

All previous publications of the BSURP are also available to view on the BSA website at https://www.bsaucalgary.ca/bsurp. We hope this publication not only showcases the fantastic work of Biological Sciences students over the years and encourages other students to get involved in research, but also provides insight into what research is about and what students can achieve.

Eligibility

To be eligible to submit to the BSURP, applicants must have been undergraduate Biological Sciences students at the University of Calgary for the duration of their projects. The project must have taken place between May 2022 and May 2024, and both research courses (e.g. 507/528/530) and non-credit projects were acceptable. Research could have occurred in any department so long as the student was a Biological Sciences student.

Contributors

The following University of Calgary undergraduate students and alumni are featured in this publication:

Kylie Jensen
Davis Dickson
Shiva Bahmanyar
Demi Ma
Ayesha Rehan

BSURP Team

Beverly Dong (2022-24 BSA Vice-President Academic) led the project and assembled the publication. The 2023-2024 Academic team (Beverly Dong, Madeline Fraser, Arya Khosravany) collaborated with design, editing, determining submission criteria, and promotion of the publication.

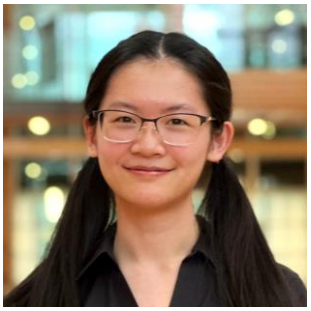

Beverly Dong

VP Academic
2022-24

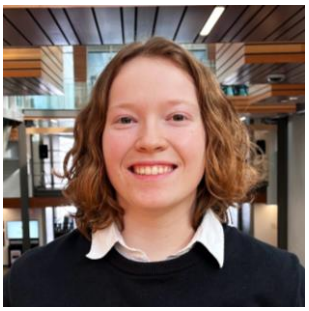

Madeline Fraser

Academic Coordinator
2022-24

Arya Khosravany

Academic Coordinator
2023-24

Acknowledgements

We would like to thank all applicants for participating in BSURP and sharing their amazing work! We hope the research experience has been one that is meaningful and sparked further interest in science. To all current and future researchers reading this publication, we hope the experiences of the wonderful individuals featured here are inspiring and enjoyable.

Additionally, we would like to thank the BSA 2023-24 executive team for helping shape this publication and assisting with logistics, feedback, and marketing.

Contact Us

The BSA is a Student Union sanctioned, departmental club at the University of Calgary that provides community engagement opportunities, academic resources, professional development events, and so much more. Our club resources and initiatives are designed to help Biological Sciences students thrive academically and professionally, connect with like-minded peers, and enhance their overall student experience. Junior and senior executive positions within the club further allows for personal development and practicing leadership. Learn more about the BSA at **bsaucalgary.ca**.

For inquiries about BSURP or the BSA, please feel free to reach out to our team at **contact@bsaucalgary.ca**.

Cover photo credits
Samples: photo by National Cancer Institute on Unsplash
White rats: photo by riccardo ragione on Unsplash
Microscope: photo by Jaron Nix on Unsplash
Macrophage: photo by National Cancer Institute on Unsplash

BSURP Research Summaries

Plasmid encoded sugar catabolism genes in the nitrogen fixing bacterium *Rhizobium leguminosarum*

Type of project: 528 (CMMB)
Supervisor(s): Dr. Michael F. Hynes

About the Researcher

Kylie Jensen

My name is Kylie Jensen and I graduated in 2023 with a BSc degree from the University of Calgary. Throughout my degree I have especially focused on courses in microbiology and infectious diseases which is what drew me to my project. I am currently working as a math/science tutor at Sylvan learning and am enrolled in a program to become a medical laboratory assistant with the hopes of going to medical school and one day becoming a doctor and working in medical research. Working in a microbiology lab this year solidified my passion for research, I enjoyed all aspects of completing this project such as learning valuable laboratory techniques like PCR and cosmid complementation, as well as meeting and interacting with a wide variety of people in the microbiology field from a range of backgrounds and education levels. If I were to give one piece of advice to someone just starting their research project, it would be to take very detailed notes. Seriously, write down every single thing you do each day, write down any results you get even the negative ones, and take photos of everything; it will save you so much hassle when you are writing your final paper. Outside of science, I love doing anything active from kayaking and hiking to strength training at the gym.

Background

Rhizobium leguminosarum is a Gram-negative alphaproteobacteria that falls into the family *Rhizobiaceae* whose members have been collectively given the name rhizobia because they all possess the ability to form a mutualistic symbiotic relationship with leguminous plants such as beans, peas, and lentils (Wielbo et al., 2007; Vanderlinde et al., 2014). In this relationship, rhizobia form nodules on plant roots and fix atmospheric nitrogen (N_2) into ammonium (NH_4) via the enzyme nitrogenase which is needed by the plants in order to grow (Wheatley et al., 2017). Rhizobia that do not exist in nodules are motile, and live freely in the nutrient rich soil that is found within close proximity of the plant roots called the rhizosphere (Vanderlinde et al., 2014; Garcia-Fraile et al., 2015). These bacteria are able to survive in the rhizosphere due to a broad range of chemicals secreted by the plant roots which can be metabolize as a carbon and energy source for rhizobia (Vanderlinde et al., 2014). This abundance of nutrients in the rhizosphere results in high interspecific competition for survival and for root occupancy to form nodules (Richardson et al., 2004) therefore placing high importance on competitive ability. It has been found that metabolic versatility, particularly the ability to utilize rare sugars as a carbon source, is the most important factor that determines competitiveness in the rhizosphere (Wielbo et al., 2007; Vanderlinde et al., 2014).

The genome of *R. leguminosarum* is large and highly complex which is one of the main reasons why this bacterium can survive in the fluctuating conditions of the rhizosphere (Stasiak et al., 2014). Aside from the main chromosome, the genome is partitioned into multiple independent replicons called plasmids which may comprise as much as 35-40% of the *Rhizobium* genome (Yip et al., 2015; Buhlers, 2019). The strain of interest in this research, VF39SM, has up to 6 plasmids that range in size from 130kb to 900kb (Zhang et al., 2001) and are denoted pRIeVF39a – pRIeVF39f in order of increasing size (Buhlers, 2019). These plasmids are not essential for survival but do confer significant competitive advantages (Buhlers, 2019) by encoding genes for chemotaxis/motility, bacteriocin production, vitamin synthesis, cell surface polysaccharide production, and carbon source utilization (Stasiak et al., 2014; Vanderlinde et al., 2014). Common substrate utilization such as glucose, glycerol, and rhamnose is a significant factor for rhizosphere survival, however, utilization of difficult substrates such as organic and amino acids is much more important to competitiveness and is generally only seen in highly competitive species (Wielbo et al., 2007; Vanderlinde et al., 2014). Currently, many plasmid encoded catabolism operons have been classified in VF39SM including the glycerol glp operon on pRIeVF39c, two ribitol operons on pRIeVF39c and pRIeVF39d, and the erythritol ery operon on pRIeVF39f.

A main goal of this research is to determine what happens to rare sugar catabolism abilities when certain plasmids are removed from *R. leguminosarum* VF39SM, to assess if the wildtype and the cured derivative strains can grow on rare sugars which like L-arabitol and D-tagatose which have not yet been tested, and finally to isolate specific genes involved in these catabolic processes and determine if these abilities ultimately affect *Rhizobium* competitiveness in the rhizosphere.

Methods

Initial tests to determine if plasmid encoded catabolism abilities were affected by plasmid loss was done by testing growth of the wildtype VF39SM and various cured strains, which are missing certain plasmids, in Robertsen's minimal media (Robertsen et al., 1981) containing 0.2% of the sugar of interest as a sole carbon source and incubated at 30°C. Curing procedures are outlined by Quandt and Hynes (1993) and Yip (2013). When needed, the following concentrations of antibiotics were added to the media: 500ug/mL streptomycin as all the VF39SM strains used with have Sm resistance, 100ug/mL neomycin, 20ug/mL gentamycin, and 5ug/mL tetracycline.

Attempts to amplify hypothetical catabolism loci in order to determine specific genes involved in these processes was done via polymerase chain reaction [PCR] using Q5 high-fidelity 2x master mix (BioLabs) with annealing temperatures calculated by BioLabs' NEB Tm calculator. This was done using a variety of primers for different loci including the *ery* locus and a hypothetical tagatose catabolism locus on pRIeVF39f, the hypothetical melibiose regulatory locus, an idonate, and beta-galactosidase polyol loci.

Attempts to isolate catabolism genes which have not yet been characterized in the wildtype, such as for L-arabitol, was done via cosmid complementation. pRK7813 cosmids were taken from the cosmid library made by Ding and others created using methods described in his paper (2012) and conjugated from the *E. coli* S17-1 mobilization strain into *R. leguminosarum* A1b4-1 which cannot normally grow on L-arabitol. The cosmids contained 35-45kb inserts of random sequences in the VF39SM genome and ~1200 samples were used resulting in nearly complete genome coverage. The mating spots were tested for their ability to grow on L-arabitol which would indicate that the cosmid contained genes involved in catabolism. Cosmids of interest were electroporated back into *R. leguminosarum* and their DNA was isolated using the EZ-10 spin column plasmid DNA miniprep kit (Bio Basic), and digested with EcoRI before imaging on an agarose gel for analysis.

Results

All of the cured *R. leguminosarum* strains outlined in table 1 were able to catabolize the following substrates: D-arabitol, D-melibiose, D-raffinose, D-trehalose, xylitol, and D-xylose; the results of which are summarized in table 2. The experiments which only showed minimal growth were re-inoculated on RMM agar plates, and these plates also showed growth thus confirming that catabolism was possible for these strains and growth wasn't just a result of nutrient carryover from the TY pre-cultures.

At low frequencies, some of the strains missing pRIeVF39c and pRIeVF39d such as A3b1-1 were found growing on ribitol control plates, which is unexpected as the ribitol catabolism loci are on these two missing plasmids. Hypothetically, the *ery* catabolism locus on pRIeVF39f may have acquired a mutation conferring the additional function of ribitol catabolism due to the high interconnectedness between these two catabolic paths, therefore attempts to amplify the wildtype and mutant *ery* locus using PCR was done in order to compare the sequence. However, all the attempts to amplify this large locus were unsuccessful (figure 1) due to off-target binding of the primers elsewhere in the genome, product overlap, or the large size of the locus in general.

The mating spots grown on L-arabitol RMM from cosmid complementation into strain A1b4-1, which cannot normally catabolize L-arabitol, revealed a number of colonies that grew with the expected wildtype morphology (figure 2) indicating these cells contained cosmids with wildtype genes involved in L-arabitol catabolism.

Experiments in D-tagatose revealed that the wildtype VF39SM can grow using this sugar, hypothetically via a catabolism locus on pRIeVF39f. Surprisingly, ABf strains missing pRIeVF39f were also able to grow on D-tagatose which is unexpected, however, Eckhardt gel results revealed that RecA recombinase activity in these strains allowed pRIeVF39f to be preserved in the genome. BAf strains which are $RecA^-$ could not grow on D-tagatose as they were completely cured of pRIeVF39f (figure 3).

Significance

The ability of cured strains to maintain catabolic ability of rare sugar substrates demonstrates the importance of genomic redundancy for survival as well as competitiveness in the rhizosphere, which is important because *Rhizobium* genomes are unstable and therefore prone to rapid change. However, these results also revealed the important implications of redundancy during experiments such as PCR as sequence similarity throughout the genome can cause off-target primer binding resulting in non-specific products. This highlights the need for long primers in order to increase specificity, but also further PCR optimization in general in order to successfully amplify

long loci, an important future direction for study of this bacterium. Finally, this research confirmed the roles of pRIeVF39c / pRIeVF39d in L-arabitol catabolism using cosmid complementation, as well as the role of pRIeVF39f in tagatose catabolism. Current studies are underway to isolate specific genes involved as well as to classify their functions, an important step towards labelling unknown genome products. In terms of broad implications, the amount of bioavailable nitrogen compounds in the rhizosphere is directly proportional to the plant shoot height (Wielbo et al., 2007), therefore nitrogen fixing *Rhizobium* species are crucial for growth and sustainability of crops we rely on for food (Goyal et al., 2021). The problem is that native soil strains are better adapted to life in the rhizosphere and therefore outcome *Rhizobium,* but are inefficient at fixing nitrogen (Goyal et al., 2021). In order to improve competitiveness of *Rhizobium* species and therefore increase crop yield, it is important to determine how rare sugars are catabolized with the hopes of producing elite strains that are highly efficient at nitrogen fixation and top competitors in specific soil conditions for ultimate use as biofertilizers (Goyal et al., 2021). This is also an important step in limiting the use of nitrogen fertilizers to prevent harmful effects of eutrophication on ecosystems.

References

Buhlers, D. (2019). Genetics of ribitol catabolism in *Rhizobium leguminosarum*. [Doctoral dissertation, University of Calgary, Calgary, AB]. Retrieved from https://prism.ucalgary.ca/items/b0afb08d-0097-4639-8ba1-50c3aca9f976.

Ding, H., Yip, C. B., Geddes, B. A., Oresnik, I. J., & Hynes, M. F. (2012). Glycerol utilization by *Rhizobium leguminosarum* requires an ABC transporter and affects competition for nodulation. *Microbiology, 158*(5), 1369-1378. http://doi.org/10.1099/mic.0.057281-0.

Garcia-Fraile, P., Seaman, J. C., Karunakaran, R., Edwards, A., Poole, P. S., & Downie, J. A. (2015). Arabinose and protocatechuate catabolism genes are important for growth of *Rhizobium leguminosarum biovar viciae* in the pea rhizosphere. *Plant and Soil, 390*(1/2), 251-264. https://doi.org/10.1007/s11104-015-2389-5.

Goyal, R. K., Schmidt, M. A., & Hynes, M. F. (2021). Molecular biology in the improvement of biological nitrogen fixation by Rhizobia and extending the scope to cereals. *Microorganisms (Basel), 9*(1), 1-24. https://doi.org/10.3390/microorganisms9010125.

Quandt, J., & Hynes, M. F. (1993). Versatile suicide vectors which allow direct selection for gene replacement in Gram-negative bacteria. *Gene, 127*(1), 15-21. https://doi.org/10.1016/0378-1119(93)90611-6.

Richardson, J. S., Hynes, M. F., & Oresnik, I. J. (2004). A genetic locus necessary for rhamnose uptake and catabolism in *Rhizobium leguminosarum bv. trifolii*. *Journal of Bacteriology, 186*(24), 8433-8422. https://doi.org/10.1128/JB.186.24.8433-8442.2004.

Robertsen, B. K., Aman, P., Darvill, A. G., McNeil, M. & Albersheim, P. (1981). Host-symbiont interactions: V. The structure of acidic extracellular polysaccharides secreted by *Rhizobium leguminosarum* and *Rhizobium trifolii*. *Plant Physiology, 67*(3), 389–400. https://doi.org/10.1104/pp.67.3.389.

Stasiak, G., Mazur, A., Wielbo, J., Marczak, M., Żebracki, K., Koper, P., & Skorupska, A. (2014). Functional relationships between plasmids and their significance for metabolism and symbiotic performance of *Rhizobium leguminosarum bv. trifolii*. *Journal of applied genetics, 55*(4), 515-527. https://doi.org/10.1007/s13353-014-0220-2.

Wheatley, R. M., Ramachandran, V. K., Geddes, B. A., Perry, B. J., Yost, C. K., & Poole, P. S. (2017). Role of O2 in the growth of *Rhizobium leguminosarum bv. viciae* 3841 on glucose and succinate. *Journal of Bacteriology, 199*(1), e00572-16. https://doi.org/10.1128/JB.00572-16.

Wielbo, J., Marek-Kozaczuk, M., Kubik-Komar, A., & Skorupska, A. (2007). Increased metabolic potential of *Rhizobium* spp. is associated with bacterial competitiveness. *Canadian Journal of Microbiology, 58*(8), 957-967. https://doi.org/10.1139/W07-053.

Vanderlinde, E. M., Hynes, M. F., & Yost, C. K. (2014). Homoserine catabolism by *Rhizobium leguminosarum bv. viciae* 3841 requires a plasmid-borne gene cluster that also affects competitiveness for nodulation. *Environmental microbiology, 16*(1), 205-217. https://doi.org/10.1111/1462-2920.12196.

Yip, C. (2013). Replication, stability, and incompatibility determinants of Rhizobium leguminosarum plasmids. [Doctoral dissertation, University of Calgary, Calgary, AB]. Retrieved from https://prism.ucalgary.ca/items/caaa8d6c-c247-4486-9d82-5063001d21ac.

Yip, C. B., Ding, H., & Hynes, M. F. (2015). Counter-transcribed RNAs of *Rhizobium leguminosarum repABC* plasmids exert incompatibility effects only when highly expressed. *Plasmid, 78*, 37-47. https://doi.org/10.1016/j.plasmid.2014.12.003.

Zhang, X. Kosier, B., & Priefer, U. B. (2001). Symbiotic plasmid rearrangement in *Rhizobium leguminosarum bv. viciae* VF39SM. *Journal of Bacteriology, 183*(6), 2141-2144. https://doi.org/10.1128/JB.183.6.2141-2144.2001.

Figures

Table 1: Summary of all the strains used in this research.

Strain	Features
R. leguminosarum bv. viciae	
VF39SM	Wildtype strain with plasmids pRIeVF39a – pRIeVF39f, Sm^r
VF39SM*	Plasmids pRIeVF39a – pRIeVF39f, *recA*$^-$, Sm^r
A1b4-1	Only has largest plasmids pRIeVF39e and pRIeVF39f, Sm^r
A3b1-1	Only has pRIeVF39e and pRIeVF39f, Sm^r
B1a2	Only has pRIeVF39e and pRIeVF39f, *recA*$^-$, Sm^r
B3a2	Only has pRIeVF39e and pRIeVF39f, *recA*$^-$, Sm^r
ABf3-1 (3-2, 3-3)	Only has pRIeVF39e, Sm^r
BAf8-1 (8-2, 8-5)	Only has pRIeVF39e, *recA*$^-$, Sm^r
E. coli	
S17.1	For conjugation, RP4 *tra* region (Buhlers, 2019)
Plasmids	
pJQ200SK (for plasmid curing)	*sacB*, Gm^r, *repABC* operon of interest
pRK7813	Tc^r, *lac* operon, VF39SM genomic insert

Table 2: Summary of the level of growth of various strains of *R. leguminosarum bv. viciae* in liquid RMM with different substrates as the sole carbon source.

Strain	Substrate						
	D-raffinose	D-melibiose	D-arabitol	D-trehalose	Xylitol	D-xylose	Dulcitol
VF39SM	Growth	Growth	Growth	Growth	Growth	Growth	Growth
VF39SM*	Growth	Growth	Growth	Growth	Growth	Growth	n.d.
A1b4-1	Growth	Growth	Growth	Growth	Growth	n.d.	n.d.
A3b1-1	Growth	Growth	Growth	Growth	Growth	n.d.	n.d.
B1a2*	Growth	Growth	Growth	Growth	Growth	n.d.	n.d.
B3a2*	Growth	Growth	Growth	Growth	Growth	n.d.	n.d.
ABf3-1	Minimal growth	Minimal growth	Minimal growth	Minimal growth	Minimal growth	Minimal growth	n.d.
BAf3-1*****	Minimal growth	Minimal growth	Minimal growth	Minimal growth	Minimal growth	Minimal growth	n.d.

*: *recA* mutant n.d.: no data (not tested)

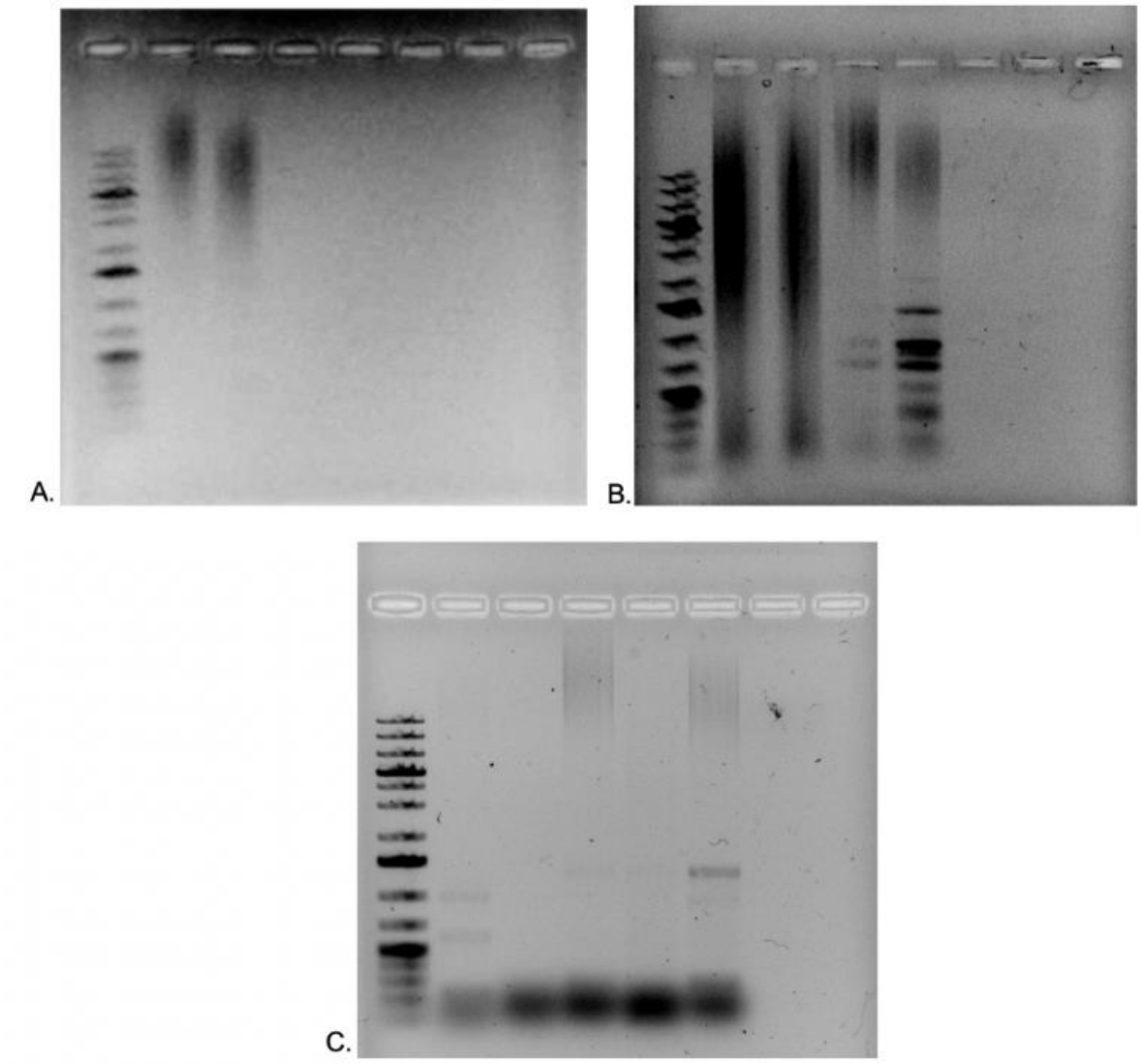

Figure 1: Agarose gel results of the PCR products containing attempted amplification of the *ery* locus in both wildtype VF39SM and A3b1-1 ribitol^{+} mutants. A) First attempt shows smudged bands around 20kb for VF39SM (lane 2) and A3b1-1 (lane 3) which matches the estimated size of the locus. B) Amplification of the *ery* locus in two parts with the additional EryMid primers. First half of the locus (lanes 2 and 3, VF39SM and A3b1-1 respectively) appeared as wide smudges in both strains while the second half (lanes 4 and 5) produced distinct bands but smaller than expected (<1000bp). C) Results of *ery* amplification using the longer primers, lane 4 is VF39SM and lane 5 and 6 are A3b1-1 ribitol^{+} mutants, all have one faint band at 1500bp suggested improved specificity but lots of unreacted primer at the bottom of the gel.

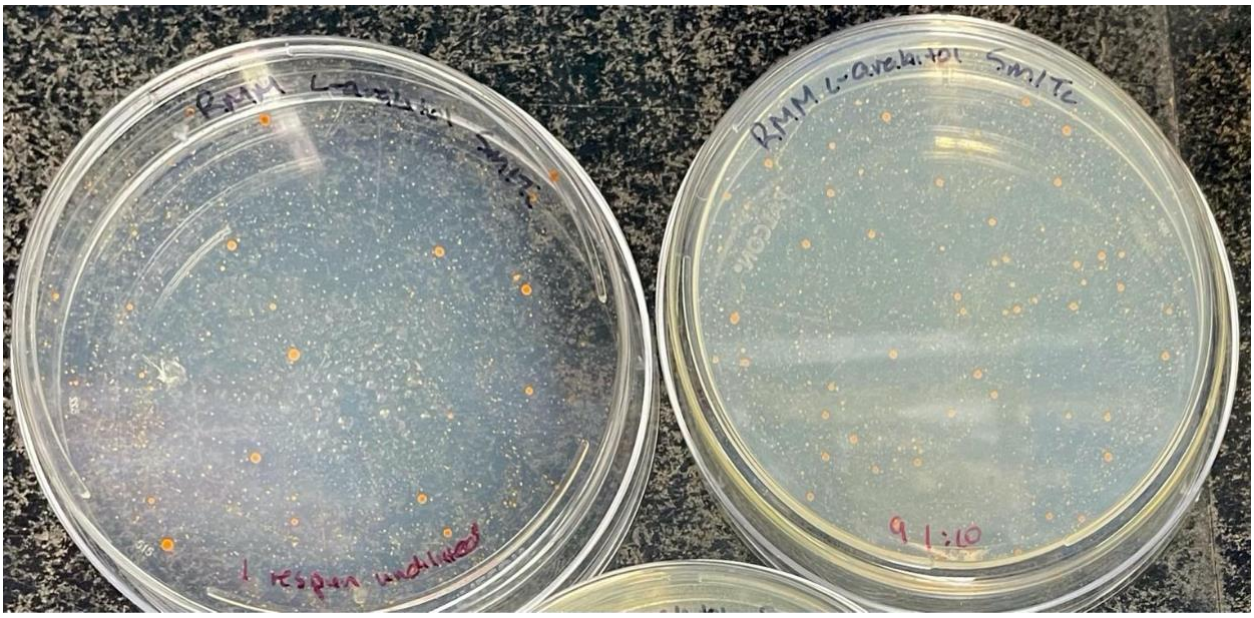

Figure 2: Colony growth of *R. leguminosarum* A1b4-1 on Sm/Tc L-arabitol RMM plates after mating with *E. coli* S17-1 to receive the cosmids. Results produced two distinct colony morphologies: majority are very small, white colonies representing cells which are not capable of growth on L-arabitol, and larger yellowish coloured colonies matching the expected phenotype for the wildtype strain suggesting these cells contain cosmids that encode L-arabitol catabolism genes.

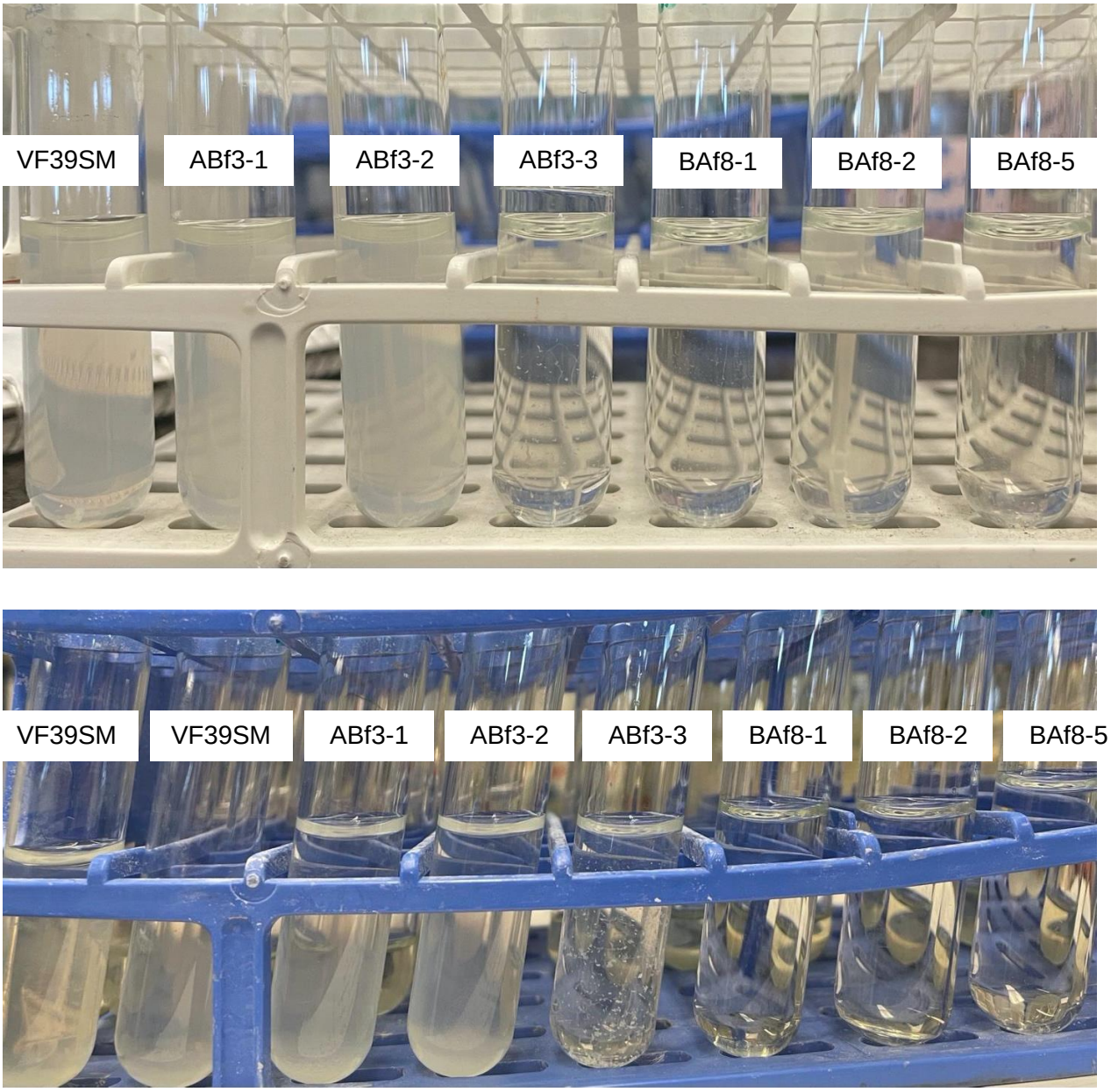

Figure 3: Level of growth of VF39SM and various cured strains in liquid RMM containing only D-tagatose as a carbon source. VF39SM as well as ABf3-1 and 3-2 tubes are turbid suggesting growth is possible in the media while the BAf tubes are clear indicating no growth occurred. ABf3-3 tubes are slightly turbid and much slower growing than the other ABf and wildtype strains as only parts of pRIeVF39f were preserved. These results are consistent across both experiments.

Investigating fibrosis in the infrapatellar fat pad of female Sprague-Dawley rats using a diet-induced obesity model

Type of project: 530 (BIOL)
Supervisor(s): Dr. Walter Herzog and Dr. Kelsey Lucas

About the Researcher

Davis Dickson

My name is Davis Dickson. I am a fourth-year honours undergraduate student, and I am hoping to pursue a career in the field of medicine! I'm interested in joints and muscles and developing ways to keep them healthy. What I enjoyed most was presenting my work. It felt very satisfying to show people what I had worked so hard on all year. Outside of science I enjoy sports, outdoors, photography, and music.

Background

Osteoarthritis (OA) is a degenerative joint disease that leads to stiffness of the joint, limited mobility, pain, and joint degeneration (Mora et al., 2016). A singular cause of OA is difficult to pin-point because it is a multifactorial disease with many factors that contribute to its development (Mora et al., 2016). Some of these factors include obesity, age, injury-related trauma, and fibrosis (Belluzzi et al., 2019; Rim & Ju, 2021). The primary focus of this study is on a specific phenotype of OA called metabolic OA which is related to obesity, systemic inflammation, and fibrosis of the infrapatellar fat pad (IFP) (Belluzzi et al., 2019; Collins et al., 2018). More specifically, we looked at the IFP in the knee joint to determine a relationship between these three factors.

Obesity has been linked to metabolic OA because it leads to dysbiosis, higher permeability of the intestinal lining and increased size of adipose stores (Collins et al., 2018; Jääskeläinen et al., 2023). Dysbiosis and increased intestinal permeability allow bacteria to escape into the bloodstream resulting in endotoxemia which can lead to systemic inflammatory secretions (Ansari et al., 2020; Collins et al., 2018). Adipocytes expand to accommodate the higher storage demands on the increased lipid content in the body (Longo et al., 2019). In response to the cellular expansion and increased secretions of adipocytes, they increase collagen production and deposition into the extracellular matrix (ECM) to limit the growth of the cells (Jääskeläinen et al., 2023; Longo et al., 2019). The increase of collagen and inflammatory secretions contribute to the development of fibrosis which leads to stiffness and pain in joints in cases of OA (Belluzzi et al., 2019; Longo et al., 2019; Rim & Ju, 2021).

The IFP sits below the patella and has many roles in the knee joint (Belluzzi et al., 2019). It is involved in structural support of the knee, healing response, and vascular supply to surrounding tissues (Belluzzi et al., 2019). It provides structural support during articular activity by distributing synovial fluid throughout the joint as well as acting like a cushion itself (Belluzzi et al., 2019). This reduces wear and tear on the joint during articular activity (Belluzzi et al., 2019).

A previous study by Rios et al. (2019) showed that feeding male rats a HFS diet supplemented with a prebiotic fibre intervention protected the knee joint from degeneration and the development of OA (Rios et al., 2019). Prebiotic fibre has been reported to bind to short chain fatty acids and stimulate hormones associated with reduction in appetite in rats (Rios et al., 2019). It also promotes gut health and reduces intestinal permeability, which reduces systemic inflammation (Rios et al., 2019). The aim of this study was to determine if these protective effects of prebiotic fibre intervention would be observed in the IFP of female Sprague-Dawley rats on a HFS diet-induced obesity model. Female rats were used to investigate any potential sex dependent differences when exposed to the diet-induced obesity model and the prebiotic fibre

intervention. We hypothesized that prebiotic fibre intervention would limit the adipocyte size increase and collagen content in the IFP that is observed in rats exposed to a high fat and high sucrose (HFS) diet. We expected to see larger adipocytes and higher collagen content in rats on the HFS diet than in rats receiving the fibre supplementation.

Methods

Thirty-two, twelve-week-old, female Sprague-Dawley rats were randomized into four diet groups: (i) a Chow control diet (n=8), (ii) a HFS diet (n=8), (iii) a HFS diet supplemented with prebiotic fibre introduced three weeks after exposure to the HFS diet (HFS+DF) (n=8), and (iv) a HFS diet supplemented with prebiotic fibre introduced at the same time as exposure to the HFS diet (HFS+STF) (n=8). The chow diet consisted of 5% of total weight as fat, 47.5% carbohydrates (only 4% from sucrose), 25% protein, 12.5% from fibre and micronutrients, and 10% moisture (Lab Diet 5001, United States). The HFS diet consisted of 20% of total weight as fat, 50% sucrose, 20% protein, and 10% from fibre and micronutrients (custom Diet #102412, Dyets, United States). Prebiotic fibre intervention was supplemented at a dose of 10% of body weight (wt/wt, Orafi P95, BENEO-Orafi, Germany). The diets were implemented at 12 weeks of age, except for the HFS+DF group, which received HFS at 12 weeks and prebiotic fibre at 15 weeks. Rats were sacrificed when they were 24 weeks old, and the knee joints were collected, cleaned from excess muscles, processed, embedded in paraffin wax to preserve the tissue, and cut into 10 μm sections using a microtome.

Knee joints were deparaffinized with Xylene and rehydrated in distilled water. One midline, sagittal section of the knee joint was selected and analyzed per rat. The sections were stained using Picro Sirius Red and then imaged using Rasa style imaging. Adipocyte size and collagen content of the IFP were determined using ImageJ (version 1.54i). Two thousand random cells were used to assess changes in adipocyte size. Adipocyte sizes were grouped into area bins of 250μm². Collagen content was determined using colour thresholding and was analyzed as a percentage of the scanned area of the IFP. Independent-Samples Kruskal-Wallis tests were conducted to detect differences between the groups ($p \leq 0.05$). Significance values were adjusted using Bonferroni correction for multiple analyses.

Results

The results for adipocyte size showed that there was no significant difference in cell size between chow and HFS+STF diet group rats in any of the bins. There were significantly more cells with an area of less than 250μm² in the chow ($p=0.003$), HFS+STF ($p=0.003$), and HFS+DF ($p=0.028$) group rats compared to the HFS group rats (Figure 1).

The HFS and HFS+DF diet groups had significantly fewer cells than chow (p=0.006, p=0.05) and HFS+STF (p=0.004, p=0.031) diet groups for cells that were within 250μm² and 500μm². Only the HFS group rats had significantly fewer cells than the chow group rats (p=0.05) for cells between 500μm² and 750μm². There was no significant difference between any of the diet groups for cells between 750μm² and 1000μm². HFS diet group rats had significantly more large cells in each bin larger than and including 1000μm² when compared to chow and HFS+STF group rats. The HFS+DF group rats had significantly more cells between 1250μm² and 1750μm² than the chow diet group rats. For cells larger than 1750μm², HFS+DF group rats had more cells than chow and HFS+STF diet groups, but these last results were not statistically significant. The overall trend of these results shows that chow and HFS+STF diet groups had fewer small adipocytes and HFS group rats had more large adipocytes. The HFS+DF diet group had an intermediate amount of small and large cells between chow and HFS diet groups (Figure 1).

Collagen content was significantly lower in HFS and HFS+DF diet groups compared to chow (p=0.022, p=0.018) and HFS+STF (p=0.011, p=0.011) diet groups. The mean collagen percentage in the chow, HFS, HFS+DF, and HFS+STF group rats was 8.5%, 5.7%, 5.7%, and 9.4% respectively. There was no significant difference between chow and HFS+STF, nor was there a significant difference between HFS and HFS+DF group rats (Figure 2). When we considered the collagen content results with the adipocyte size results in a linear regression, there was a negative relationship between the percentage of collagen in the IFP and the size of the adipocytes (p=0.009) (Figure 3).

Significance

The results for adipocyte size are consistent with other studies showing adipocyte expansion in obese conditions in rats (Jääskeläinen et al., 2023; Longo et al., 2019). Rats on the HFS had the highest number of large cells and chow and HFS+STF diets had the fewest, as expected. The high fat and sugar content in the HFS diet led to the expansion of the adipocytes in the IFP. However, the prebiotic fibre intervention prevented this effect in a time dependent manner. The same-time prebiotic fibre intervention group rats and chow control group rats had a similar number of cells in each cell area bin, indicating that the prebiotic fibre intervention sufficiently protected the adipose tissue from adipocyte expansion when exposed to the HFS diet. However, the delayed prebiotic fibre had an increased number of large cells compared to the chow and HFS+STF group rats.

Even though the increase of large adipocytes in HFS+DF group rats was not statistically significant, it indicates that the delayed prebiotic fibre intervention provides some level of protection against obesity-induced changes in the IFP. This result shows that the timing of the fibre intervention is important for preventing changes induced by obesity. In a study by Yang et al. (2012) there were significant changes in white adipose

tissue of mice within 2 weeks of administering a HFS diet. With such rapid changes in the tissues and metabolism of these animals on the HFS diet, it is likely that the three-week period in which the HFS+DF group rats were on the HFS diet without the fibre supplementation led to irreversible changes (Collins et al., 2018; Yang et al., 2012).

The collagen content in the IFP of chow and HFS+STF diet group rats was unexpected. In comparison to the chow and HFS+STF group rats, the collagen content in HFS and HFS+DF group rats was lower. This result is inconsistent with the literature (Jääskeläinen et al., 2023; Longo et al., 2019; Zeng et al., 2020). We expected to see higher collagen content in HFS and HFS+DF group rats. This was the expectation because the local inflammation caused by increased adipocyte size has been shown to be correlated with higher levels of fibrosis in adipose tissue (Jääskeläinen et al., 2023; Longo et al., 2019; Zeng et al., 2020). One reason for the unexpected result of collagen content could be that the relative area occupied by adipocytes in the scanned images of the IFP was disproportionately increased compared to collagen content. If it was assumed that collagen content in the IFP increased at a slower rate than the cells grew, then the area of collagen would appear to be less (Figure 4). There is also the possibility that the collagen content per cell increased but was overshadowed by the increase in mean cell size (Liu et al., 2020; Longo et al., 2019).

References

Ansari Saleem, Haboubi Hansan, H. N. (2020). Adult obesity complications: challenges and clinical impact. *Therapeutic Advances in Endocrinology and Metabolism*, *11*, 1–14. https://doi.org/10.1177/2042018820934955

Belluzzi, E., Stocco, E., Pozzuoli, A., Granzotto, M., Porzionato, A., Vettor, R., De Caro, R., Ruggieri, P., Ramonda, R., Rossato, M., Favero, M., & MacChi, V. (2019). Contribution of Infrapatellar Fat Pad and Synovial Membrane to Knee Osteoarthritis Pain. *BioMed Research International*, *2019*. https://doi.org/10.1155/2019/6390182

Chang W., DeMoe J., Kent C., Kovats S., Garteiser P., Doblas S., Towner R., Griffin T. (2011). Infrapatellar fat pad hypertrophy without inflammation in a diet-induced mouse model of obesity and osteoarthritis. *Osteoarthritis and Cartilage*. *19*(566).

Collins, K. H., Herzog, W., MacDonald, G. Z., Reimer, R. A., Rios, J. L., Smith, I. C., Zernicke, R. F., & Hart, D. A. (2018). Obesity, metabolic syndrome, and musculoskeletal disease: Common inflammatory pathways suggest a central role for loss of muscle integrity. *Frontiers in Physiology*, *9*(FEB). https://doi.org/10.3389/fphys.2018.00112

Jääskeläinen, I., Petäistö, T., Mirzarazi Dahagi, E., Mahmoodi, M., Pihlajaniemi, T., Kaartinen, M. T., & Heljasvaara, R. (2023). Collagens Regulating Adipose Tissue Formation and Functions. *Biomedicines*, *11*(5), 1–21. https://doi.org/10.3390/biomedicines11051412

Jiang, L. F., Fang, J. H., & Wu, L. D. (2019). Role of infrapatellar fat pad in pathological process of knee osteoarthritis: Future applications in treatment. *World Journal of Clinical Cases*, *7*(16), 2134–2142. https://doi.org/10.12998/wjcc.v7.i16.2134

Liu, F., He, J., Wang, H., Zhu, D., & Bi, Y. (2020). Adipose Morphology: a Critical Factor in Regulation of Human Metabolic Diseases and Adipose Tissue Dysfunction. *Obesity Surgery*, *30*(12), 5086–5100. https://doi.org/10.1007/s11695-020-04983-6

Longo, M., Zatterale, F., Naderi, J., Parrillo, L., Formisano, P., Raciti, G. A., Beguinot, F., & Miele, C. (2019). Adipose tissue dysfunction as determinant of obesity-associated metabolic complications. *International Journal of Molecular Sciences*, *20*(2358). https://doi.org/10.3390/ijms20092358

Mora, J. C., Przkora, R., & Cruz-Almeida, Y. (2018). Knee osteoarthritis: Pathophysiology and current treatment modalities. *Journal of Pain Research*, *11*, 2189–2196. https://doi.org/10.2147/JPR.S154002

Parnell, J. A., & Reimer, R. A. (2012). Prebiotic fiber modulation of the gut microbiota improves risk factors for obesity and the metabolic syndrome. *Gut Microbes*, *3*(1), 29–34. https://doi.org/10.4161/gmic.19246

Rim, Y. A., & Ju, J. H. (2021). The role of fibrosis in osteoarthritis progression. *Life*, *11*(3), 1–13. https://doi.org/10.3390/life11010003

Rios, J. L., Bomhof, M. R., Reimer, R. A., Hart, D. A., Collins, K. H., & Herzog, W. (2019). Protective effect of prebiotic and exercise intervention on knee health in a rat model of diet-induced obesity. *Scientific Reports*, *9*(1), 1–10. https://doi.org/10.1038/s41598-019-40601-x

Santangelo, K. S., Radakovich, L. B., Fouts, J., & Foster, M. T. (2016). Pathophysiology of obesity on knee joint homeostasis: Contributions of the infrapatellar fat pad. *Hormone Molecular Biology and Clinical Investigation*, *26*(2), 97–108. https://doi.org/10.1515/hmbci-2015-0067

Wynn, T. (2009). Cellular and molecular mechanisms in fibrosis. *National Institutes of Health*, *214*(2), 199–210. https://doi.org/10.1002/path.2277

Yang, Z., Miyahara, H., Takeo, J., & Katayama, M. (2012). Diet high in fat and sucrose induces rapid onset of obesity-related metabolic syndrome partly through rapid response of genes involved in lipogenesis, insulin signalling and inflammation in mice. *Diabetology & Metabolic Syndrome*, *4*, 1–10.

Zeng, N., Yan, Z. P., Chen, X. Y., & Ni, G. X. (2020). Infrapatellar fat pad and knee osteoarthritis. *Aging and Disease*, *11*(5), 1317–1328. https://doi.org/10.14336/AD.2019.1116

Figures

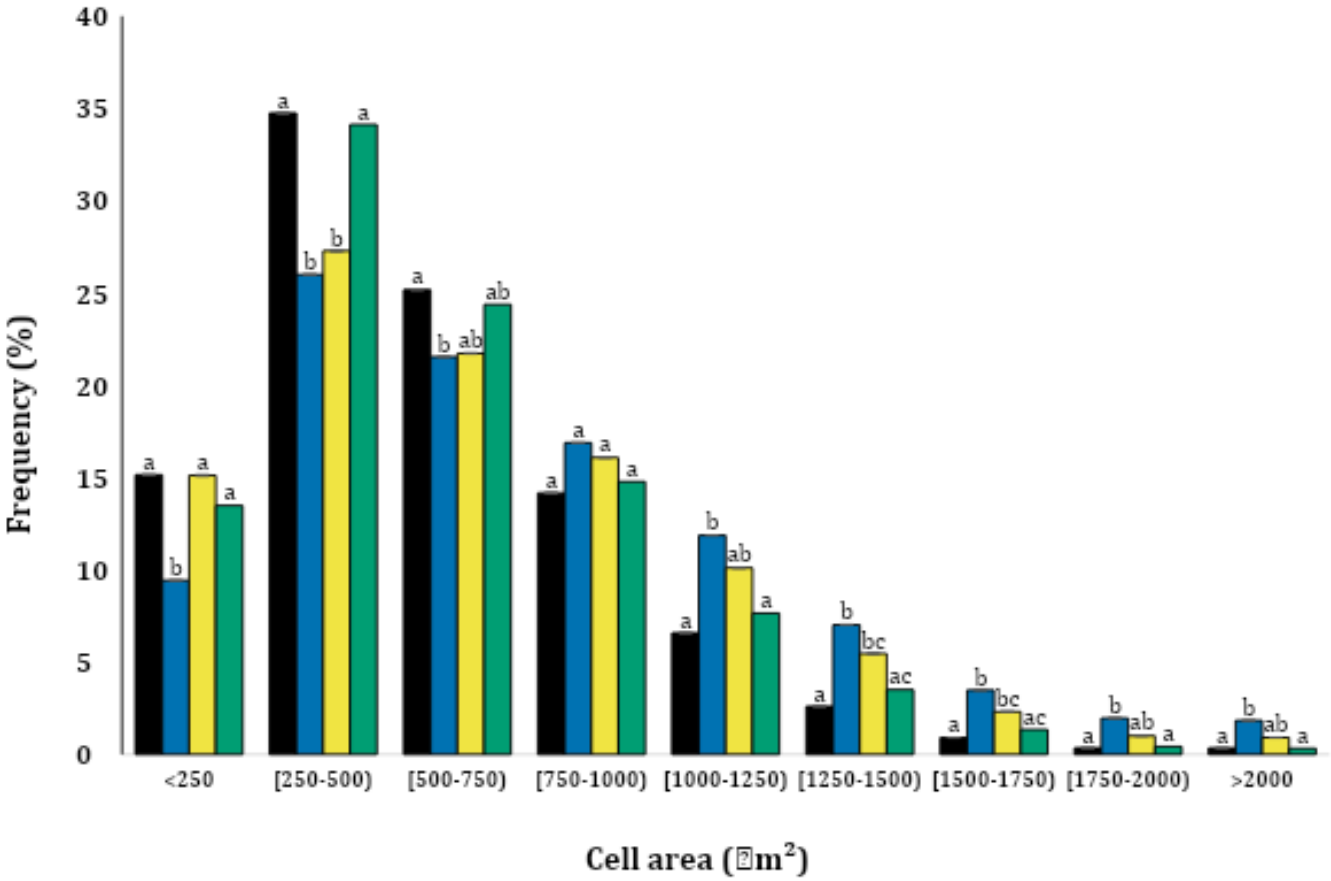

Figure 1. Frequency (%) of cells in defined cell areas (μm²) for chow (black, n=8), HFS (blue, n=8), HFS+DF (yellow, n=8), and HFS+STF (green, n=8) group rats. The cell areas are defined by bins from smaller than 250μm² to larger than 2000μm², increasing by increments of 250μm². Different letters indicate statistically significant difference between groups ($p<0.05$); same letters indicate non-statistically significant difference.

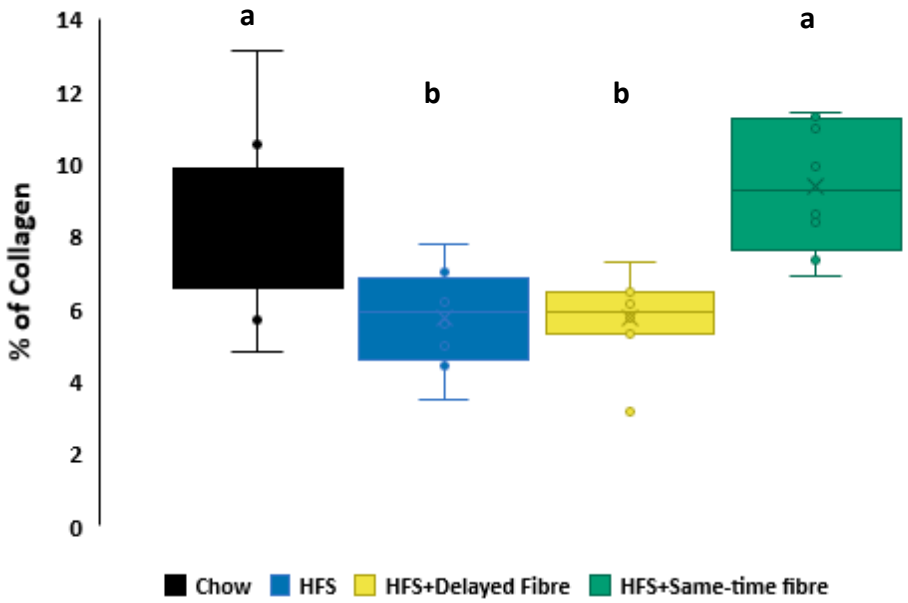

Figure 2. Box-and-whisker plot of the percentage of collagen in chow (black, n=8), HFS (blue, n=8), HFS+DF (yellow, n=8), and HFS+STF (green, n=8) group rats. Different letters indicate statistically significant difference ($p<0.05$) between groups; same letters indicate not statistically significant.

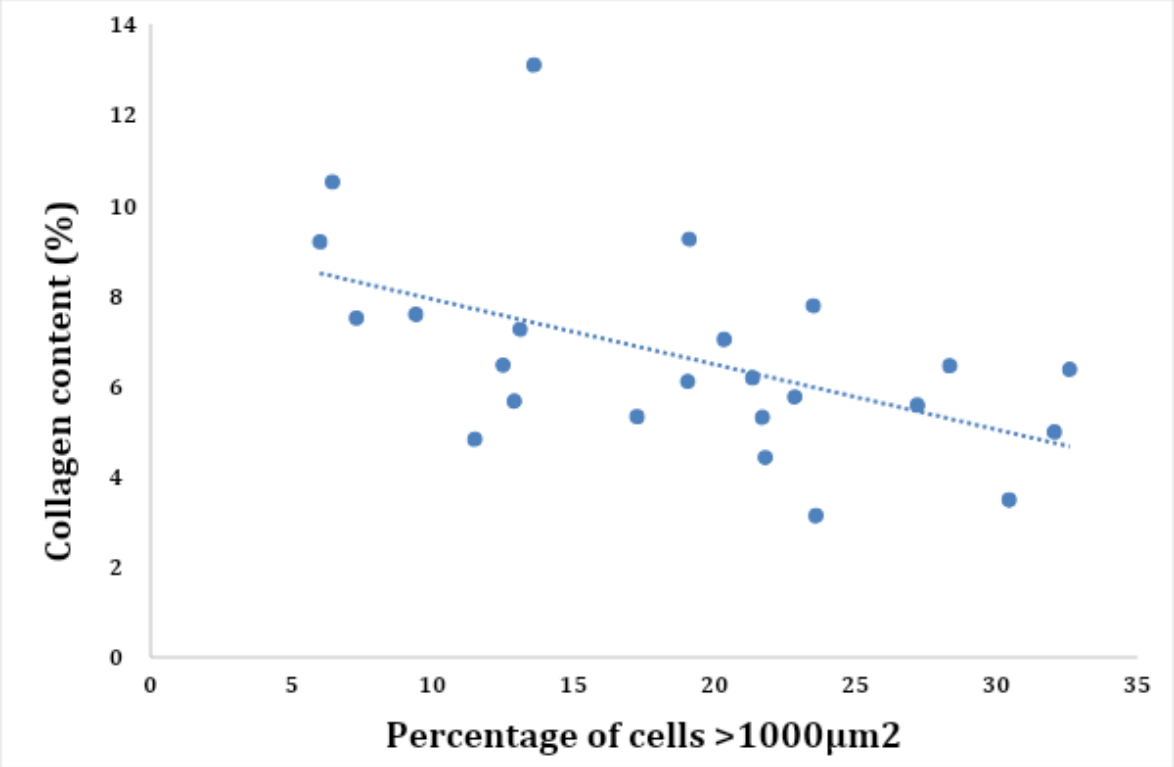

Figure 3. Linear regression of collagen content percentage and the percentage of cells with an area larger than 1000µm².

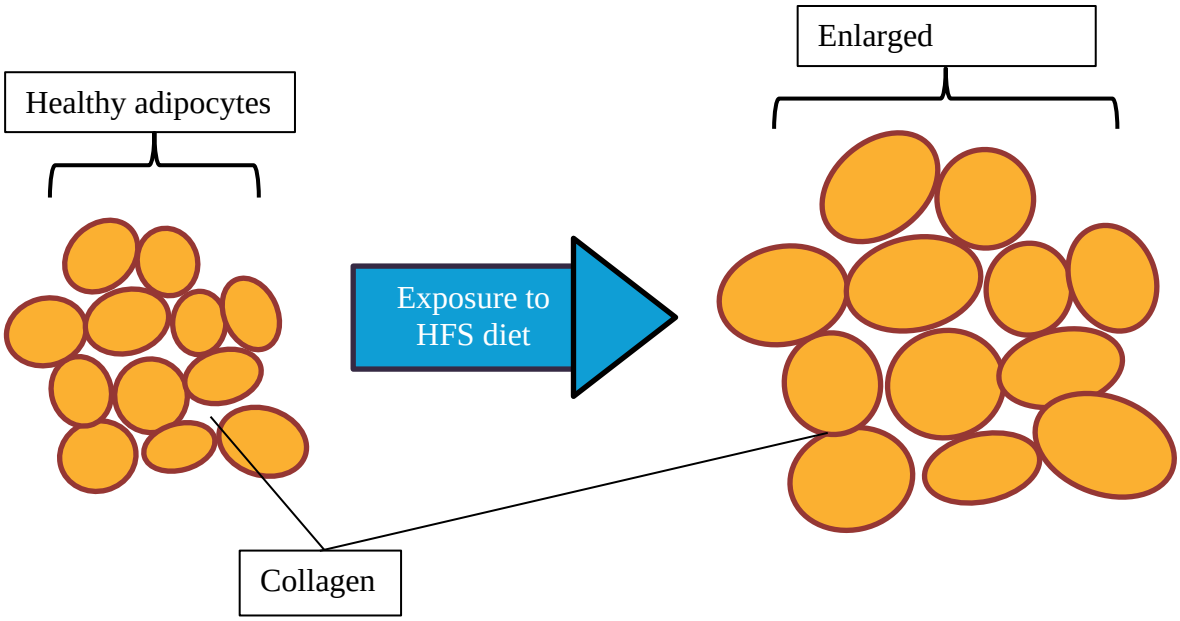

Figure 4. Healthy and enlarged adipocytes with constant collagen content in both clusters of adipocytes. When adipocyte size increases, then the collagen takes up less of the relative area, but it is still the same amount of collagen.

Where to find more about the project?

Link to my full thesis: https://1drv.ms/w/s!ArAu5q1bIcX_hjPhbd556wRiWjZU?e=PuR6lT

Inhibitory Effects of Photothermal Therapy Using Gold Nanoparticles on *Candida albicans*

Type of project: Summer / 507.01 and 507.02 (BIOL)
Supervisor(s): Dr. Elmar Prenner and Dr. Stephen Lane

About the Researcher

Shiva Bahmanyar

My Name is Shiva Bahmanyar, I am a third-year Biological Science student at the University of Calgary with a deep passion for understanding all aspects of life and nature. As a pet lover, I appreciate the time spent with animals and believe they significantly enhance our understanding and appreciation of the natural world. My academic pursuits are motivated by my interest in biological systems and my desire to make a positive impact on future scientific discoveries and innovations.

Abstract

This study investigates the potential of gold nanoparticles (AuNPs) in the photothermal treatment of fungal infections, specifically Candida albicans, which cause health challenges, especially in immunocompromised individuals. Photothermal therapy is a potential alternative to current treatments that are limited by drug resistance and their harmful side effects. Through a series of experiments, this research evaluates the success of AuNPs in inhibiting fungal growth when activated by green LED light. The main result of this study is that AuNPs, inhibit the growth of Candida albicans, when these particles are combined with green LED light. This result challenges the current antifungal treatments, providing an alternative method for managing fungal infections that may reduce their potential side effects and avoid current issues with drug resistance.

This study offers an outline for future research into the potential use of AuNPs in healthcare for different infections. Additional research is required to maximize the treatment benefits of photothermal therapy using AuNPs.

Background

Fungi

Fungi, a distinct classification of living organisms, stand apart from plants, animals, and bacteria. These unique organisms have their own kingdom in the classification of life, and have a range of forms, being either unicellular, like yeasts, which are only a few micrometers in size, or complex multicellular structures such as the vast mycelial mats of the honey mushroom, the largest known organism on Earth (Adamatzky, 2018). Fungi are heterotrophic organisms, similar to mammals, as they depend on external resources for survival, unlike plants which typically synthesize their own food through photosynthesis (Naranjo-Ortiz & Gabaldón, 2019). While some are useful to humans, like those that produce penicillin (Clardy et al., 2009), others, like Candida albicans, Aspergillus fumigatus, and Cryptococcus neoformans could be harmful (Spampinato & Leonardi, 2013b).

Fungal infections

Fungal infections are classified into four types based on their location and the body's reaction to the fungus. They are classified as superficial (mild infections that impact the surface layers of the skin or mucous membranes), cutaneous (infections that go deeper than superficial mycoses, affecting both the skin, hair, and nails), subcutaneous (expands beyond the outer layers to the subcutaneous tissue, a layer of fat and tissue that contains bigger blood vessels and nerves), or systemic (deep infections that affect internal organs and spread through the bloodstream). These infections can spread

through direct contact with infected people or by contact with contaminated objects (Walsh & Dixon, 2012).

In healthy individuals, strong immune systems naturally control fungal infections (Drummond et al., 2014). However, those with compromised immunity, such as transplant recipients and people with diabetes, face greater challenges in fighting fungal infections. Transplant medications suppress immune responses to prevent organ rejection, increasing susceptibility to infections (Hussain & Khan, 2022). High glucose levels in diabetics impair immune defenses, increasing infection risks (Berbudi et al., 2020).

Antifungals

Antifungal medicines treat a variety of fungal infections that can affect the skin, nails, mouth, and internal organs (Bryant, 2017). These medications work through different mechanisms. For instance, polyenes, such as amphotericin B, bind to ergosterol (the primary sterol in fungal cell membranes that regulates their permeability and fluidity (Douglas & Konopka, 2014)) in the fungal cell membrane, creating pores in the cell membrane. This disruption results in the leakage of cellular contents, leading to cell death (Turecka et al., 2018). Azole antifungals, such as fluconazole and ketoconazole, inhibit the fungal enzyme 14α-demethylase, essential for ergosterol synthesis, causing a breakdown of the membrane (Odds et al., 2003).

Antifungal drugs are essential for managing fungal infections but often come with side effects that vary depending on the patient's age, immune status, infection location, and severity. Common side effects of topical antifungals include skin irritation, redness, and a burning sensation at the application site. Oral antifungals, meanwhile, can lead to systemic issues such as nausea, vomiting, diarrhea, stomach pain, and liver enzyme problems (Ivanov et al., 2022) (Elewski & Tavakkol, 2005).

Another concern is antifungal resistance, which occurs when genetic mutations in a fungal pathogen make a specific class of antifungal drug less effective, leading to a higher likelihood of unsuccessful treatment (Arastehfar et al., 2020). Overuse and misuse of antifungals could result in antifungal resistance (World Health Organization, n.d.), causing infections harder to treat and leading to higher medical costs, longer hospital stays, and increased mortality (Prestinaci et al., 2015).

Nanoparticles

Nanoparticles are tiny materials with sizes ranging from 1 to 100 nm (Khan et al., 2017). They can be categorized into different classes based on their properties, shapes, or sizes. The different groups include fullerenes, metal NPs, ceramic NPs, and polymeric NPs (Khan et al., 2017). Nanoparticles have unique physical and chemical properties due to their high surface area and nanoscale size. The colors of nanoparticles vary depending

on their size, as size influences their absorption properties in the visible spectrum (Khan et al., 2017).

Gold nanoparticles (AuNPs) in particular, have shown antifungal activity against various Candida species, including drug-resistant strains (Ayad Kareem et al., 2021b). The size-dependent effects of AuNPs play a crucial role, with smaller nanoparticles (7-15 nm) demonstrating higher surface area and stronger antifungal effectiveness compared to larger AuNPs (Ensieh Lotfali et al., 2020) (Ahmad et al., 2013).

Recent studies have showed the potential of gold nanoparticles in photothermal therapies, especially in controlling and minimizing the spread of fungal infections. It has been shown that using gold nanoparticles combined with photosensitizers greatly improves the inactivation of C. albicans in photodynamic therapy (Sherwani et al., 2015). These nanoparticles enhance the delivery and activation of photosensitizers, chemical compounds that when activated by light at specific wavelengths produce reactive oxygen species (ROS) such as free radicals and singlet oxygen. The generated ROS are highly reactive and capable of damaging molecules, including damaging the cell wall integrity of the fungi (Sherwani et al., 2015).

The minimum inhibitory concentrations (the lowest concentration of an antibacterial agent expressed in mg/L (µg/mL) (Kowalska-Krochmal & Dudek-Wicher, 2021)) of AuNPs have been shown to vary significantly depending on particle size, concentration, and fungal species that were used. AuNPs at 40.77 ng/ml were shown to be the MIC for inhibiting Candida albicans using agar well diffusion methods (Ayad Kareem et al., 2021). Other methods like broth microdilution have been used to determine MICs for different sizes and concentrations of AuNPs, showing a MIC as low as 0.5 mM for some nanoparticles (Nidhin M et al., 2019).

Methods

At first for preparing agar for fungal growth, 200 mg of agar was measured and added to a 20 ml glass vial. Then, 10 ml of distilled water was added into the vial with a pipette, and the mixture was stirred. The solution was sterilized in an autoclave using standard sterilization settings (temperature of 121 degrees Celsius and a pressure of 15 psi) for 30 minutes. After sterilization, the agar solution was cooled before being poured into sterile polycarbonate Petri dishes. The Petri dishes were set aside on the counter to allow the agar to solidify completely.

The revival process for Candida albicans began with the opening of the ampoule containing the fungal pellet. 0.5 to 1.0 mL of sterile distilled water was taken out of a test tube and placed into the pellet. The solution was vortexed and poured back into the original test tube containing the leftover distilled water. The test tube was left to sit at room

temperature (approximately 25°C) undisturbed for a minimum of 2 hours. After making sure that the suspension was well-mixed by vortexing it, several drops were added to the agar media and was left undisturbed for 3 days.

For the main experiment, the antifungal properties of gold nanoparticles (AuNPs) against four samples of Candida albicans cultured in broth media were examined (Table 1).

Results

The optical density at 600 nm (OD600) was used to track growth and graphing the data over time showed initial readings of negative absorbance values (Figure 2,3,4, and 5) likely due to calibration issues or baseline drift of the spectrophotometer. Despite this, the overall trend illustrates a clear increase in absorbance over time, indicating fungal growth. A significant increase in OD600 was noted, particularly after the 1200-minute mark, where the values rose to 1.348, 1.690, 1.825, and 1.932 for each plate, respectively. By 1260 minutes, these numbers had risen to 1.395, 1.727, 1.861, and 1.954, indicating growth. Plate 1 treated with both AuNPs, and light demonstrated the greatest growth inhibition, with a rise in absorbance from 0 at time zero to 1.395 at 1260 minutes (Figure 2). Plate 2, which had only AuNPs, revealed some inhibition, with absorbance values rising from 0 to 1.727 (Figure 3). Fungal growth was slightly inhibited on Plate 3, which was exposed to light but did not contain any gold nanoparticles (AuNPs); the absorbance increased to 1.861 (Figure 4). In contrast, Plate 4, which served as the control and was not exposed to any treatment, had an absorbance of up to 1.954 (Figure 5).

Significance

In summary, this research showed that gold nanoparticles (AuNPs) are a possible treatment option for treating fungal infections, with a focus on Candida albicans. The performed experiments demonstrate the inhibitory effects of AuNPs, particularly when used in combination with photothermal therapy, demonstrating their ability to limit the growth of fungi. These results demonstrate the potential of AuNPs in healthcare settings, especially as a substitute for traditional antifungal medications that frequently cause serious side effects and a high risk of resistance. Future research should improve nanoparticle characteristics and explore how they combine with other treatments to establish a strong, effective, and safe antifungal treatment.

References

Adamatzky, A. (2018). Towards fungal computer. Interface Focus, 8(6), 20180029. https://doi.org/10.1098/rsfs.2018.0029

Ahmad, T., Wani, I. A., Lone, I. H., Ganguly, A., Manzoor, N., Ahmad, A., Ahmed, J., & Al Shihri, A. S. (2013). Antifungal activity of gold nanoparticles prepared by solvothermal method. Materials Research Bulletin, 48(1), 12–20. https://doi.org/10.1016/j.materresbull.2012.09.069

Arastehfar, A., Gabaldón, T., Garcia-Rubio, R., Jenks, J. D., Hoenigl, M., Salzer, H. J. F., Ilkit, M., Lass-Flörl, C., & Perlin, D. S. (2020). Drug-Resistant Fungi: An Emerging Challenge Threatening Our Limited Antifungal Armamentarium. Antibiotics, 9(12), 877. https://doi.org/10.3390/antibiotics9120877

Ayad Kareem, H., Mahmood Samaka, H., & Mohamed Abdulridha, W. (2021). Evaluation of the gold nanoparticles prepared by green chemistry in the treatment of cutaneous candidiasis. Current Medical Mycology. https://doi.org/10.18502/cmm.7.1.6176

Berbudi, A., Rahmadika, N., Cahyadi, A. I., & Ruslami, R. (2020). Type 2 Diabetes and Its Impact on the Immune System. Current Diabetes Reviews, 16(5), 442–449. https://doi.org/10.2174/1573399815666191024085838

Bryant, M. (2017). Fungal infections. InnovAiT: Education and Inspiration for General Practice, 10(7), 417–424. https://doi.org/10.1177/1755738017706093

Clardy, J., Fischbach, M. A., & Currie, C. R. (2009). The natural history of antibiotics. Current Biology, 19(11), R437–R441. https://doi.org/10.1016/j.cub.2009.04.001

Douglas, L. M., & Konopka, J. B. (2014). Fungal Membrane Organization: The Eisosome Concept. Annual Review of Microbiology, 68(1), 377–393. https://doi.org/10.1146/annurev-micro-091313-103507

Drummond, R. A., Gaffen, S. L., Hise, A. G., & Brown, G. D. (2015). Innate Defense against Fungal Pathogens. Cold Spring Harbor Perspectives in Medicine, 5(6). https://doi.org/10.1101/cshperspect.a019620

Elewski, B., & Tavakkol, A. (2005). Safety and tolerability of oral antifungal agents in the treatment of fungal nail disease: a proven reality. Therapeutics and Clinical Risk Management, 1(4), 299–306. https://www.ncbi.nlm.nih.gov/pmc/articles/PMC1661633/

Ensieh Lotfali, Hossein Toreyhi, Kamyab Makhdoomi Sharabiani, Fattahi, A., Amirali Soheili, Ghasemi, R., Mahyar Keymaram, Yasaman Rezaee, & Sayna Iranpanah. (2020). Comparison of Antifungal Properties of Gold, Silver, and Selenium Nanoparticles AgainstAmphotericin B-Resistant Candida glabrata Clinical Isolates. Avicenna Journal of Medical Biotechnology. https://doi.org/10.18502/ajmb.v13i1.4578

Hussain, Y., & Khan, H. (2022). Immunosuppressive drugs. Encyclopedia of Infection and Immunity, 4, 726–740. https://doi.org/10.1016/b978-0-12-818731-9.00068-9

Ivanov, M., Ćirić, A., & Stojković, D. (2022). Emerging Antifungal Targets and Strategies. International Journal of Molecular Sciences, 23(5), 2756. https://doi.org/10.3390/ijms23052756

Khan, I., Saeed, K., & Khan, I. (2017). Nanoparticles: Properties, applications and toxicities. Arabian Journal of Chemistry, 12(7), 908–931. https://doi.org/10.1016/j.arabjc.2017.05.011

Kowalska-Krochmal, B., & Dudek-Wicher, R. (2021). The minimum inhibitory concentration of antibiotics: Methods, interpretation, clinical relevance. Pathogens, 10(2), 165. https://doi.org/10.3390/pathogens10020165

M, N., D, S., Hans, S., Varghese, A., Fatima, Z., & Hameed, S. (2019). Studies on the antifungal activity of biotemplated gold nanoparticles over Candida albicans. Materials Research Bulletin, 119, 110563. https://doi.org/10.1016/j.materresbull.2019.110563

Naranjo-Ortiz, M. A., & Gabaldón, T. (2019). Fungal evolution: diversity, taxonomy, and phylogeny of the Fungi. Biological Reviews, 94(6), 2101–2137. https://doi.org/10.1111/brv.12550

Odds, F. C., Brown, A. J. P., & Gow, N. A. R. (2003). Antifungal agents: mechanisms of action. Trends in Microbiology, 11(6), 272–279. https://doi.org/10.1016/s0966- 842x(03)00117-3

Prestinaci, F., Pezzotti, P., & Pantosti, A. (2015). Antimicrobial resistance: a global multifaceted phenomenon. Pathogens and Global Health, 109(7), 309–318. https://doi.org/10.1179/2047773215y.0000000030

Sherwani, Mohd. A., Tufail, S., Khan, A. A., & Owais, M. (2015b). Gold Nanoparticle Photosensitizer Conjugate Based Photodynamic Inactivation of Biofilm Producing Cells: Potential for Treatment of C. albicans Infection in BALB/c Mice. *PLOS ONE*, *10*(7), e0131684. https://doi.org/10.1371/journal.pone.0131684

Spampinato, C., & Leonardi, D. (2013). CandidaInfections, Causes, Targets, and Resistance Mechanisms: Traditional and Alternative Antifungal Agents. BioMed Research International, 2013, 1–13. https://doi.org/10.1155/2013/204237

Turecka, K., Chylewska, A., Kawiak, A., & Waleron, K. F. (2018). Antifungal Activity and Mechanism of Action of the Co(III) Coordination Complexes With Diamine Chelate Ligands Against Reference and Clinical Strains of Candida spp. Frontiers in Microbiology, 9. https://doi.org/10.3389/fmicb.2018.01594

Khan, I., Saeed, K., & Khan, I. (2017). Nanoparticles: Properties, applications and toxicities. Arabian Journal of Chemistry, 12(7), 908–931. https://doi.org/10.1016/j.arabjc.2017.05.011

Walsh, T. J., & Dixon, D. M. (2012). Spectrum of Mycoses. Nih.gov; University of Texas Medical Branch at Galveston. https://www.ncbi.nlm.nih.gov/books/NBK7902/

World Health Organization. (n.d.). Antimicrobial resistance (AMR) is a global health and development threat. It requires urgent multisectoral action in order to achieve the Sustainable Development Goals (SDGs). https://www.who.int/docs/default source/antimicrobial-resistance/amr-factsheet.pdf

Figures

	LED Light	No Light
10 nm Gold Nanoparticles	Sample #1	Sample #2
No Gold	Sample #3	Sample #4

Table 1.0 shows the experimental setup for testing the effect of green LED light exposure on samples with and without gold nanoparticles. The experiment is divided into four sections, with samples #1 and #3 subjected to LED light and samples #2 and #4 kept without light exposure. It is possible to compare the effects of light and the presence of nanoparticles because samples #1 and #2 have 10 nm gold nanoparticles while samples #3 and #4 do not.

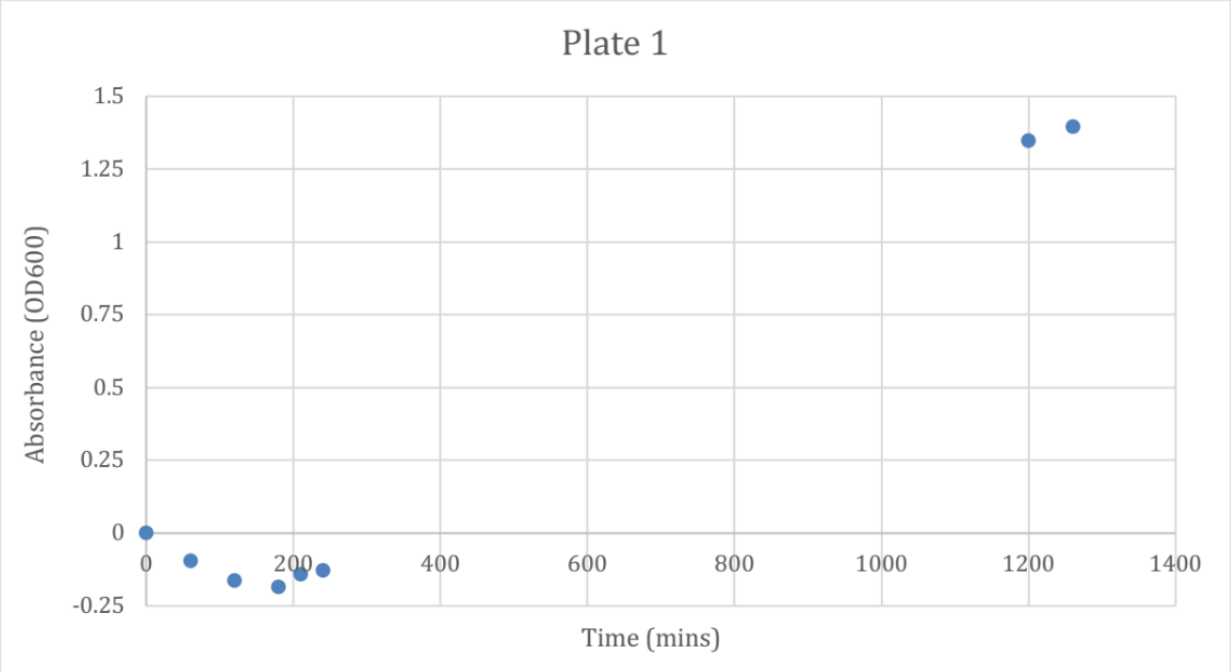

Figure 1.0 Growth curve of Candida albicans in Plate 1, showing optical density at 600 nm (OD600) over time in minutes.

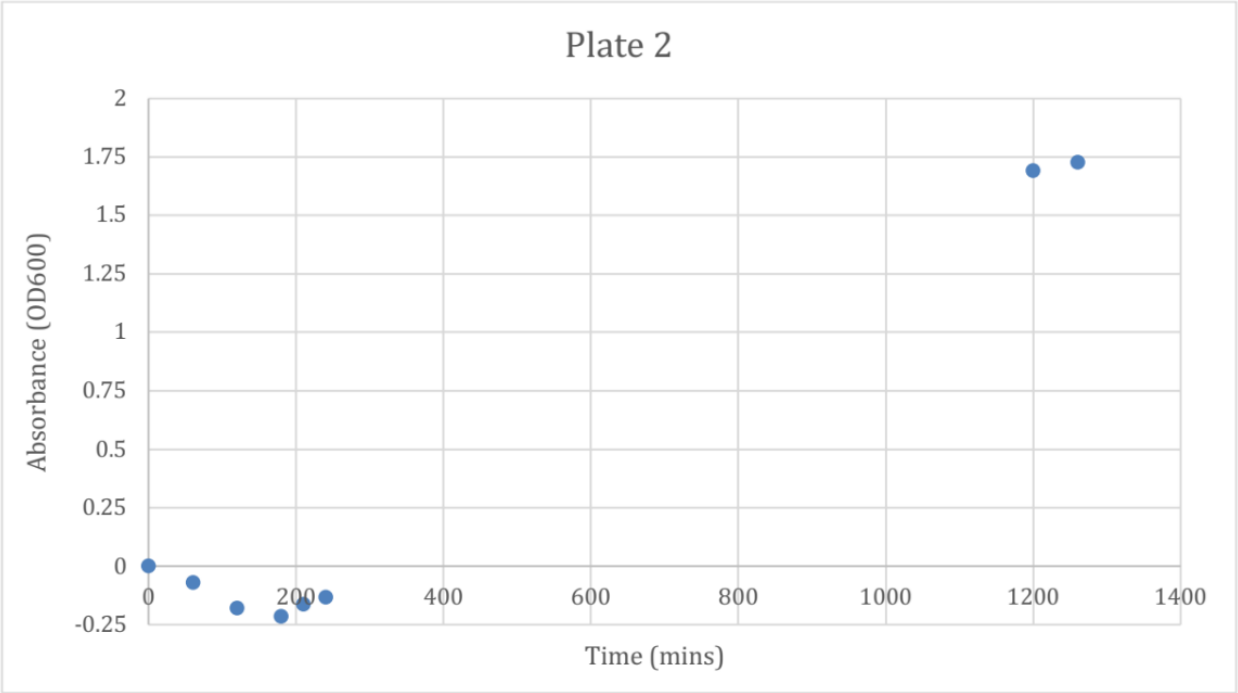

Figure 2.0 Growth curve of Candida albicans in Plate 2, showing optical density at 600 nm (OD600) over time in minutes.

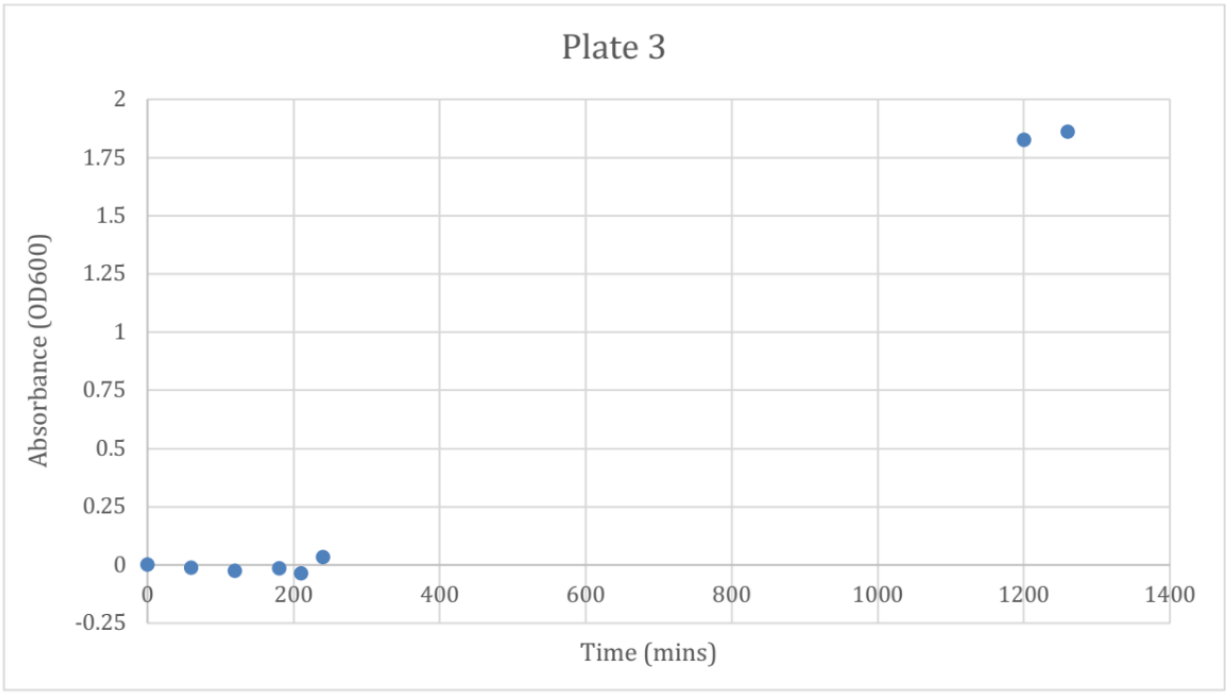

Figure 3.0 Growth curve of Candida albicans in Plate 3, showing optical density at 600 nm (OD600) over time in minutes.

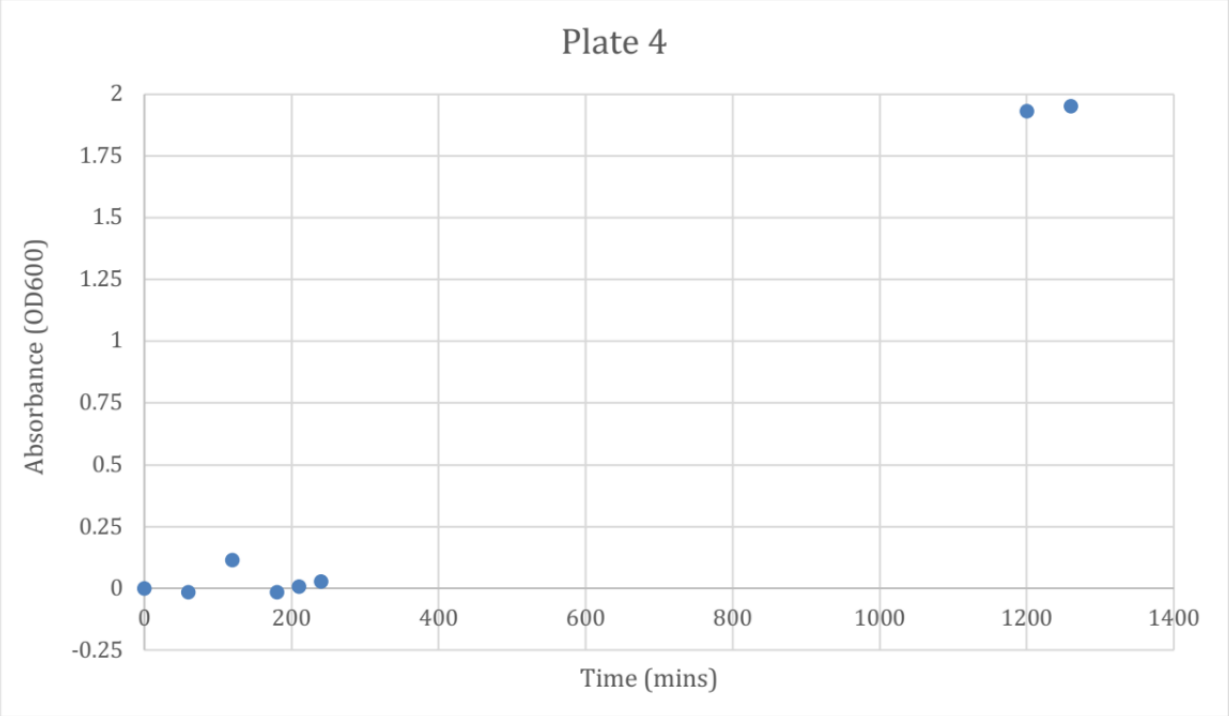

Figure 4.0 Growth curve of Candida albicans in Plate 4, showing optical density at 600 nm (OD600) over time in minutes.

BSURP Abstracts and Posters

Investigating the effects of selective inhibition of ERK signaling on protein synthesis in a mouse model of Fragile X Syndrome

Type of project: Summer
Supervisor(s): Dr. Ning Cheng

About the Researcher

Demi Ma

I am a third-year undergraduate of Biological Sciences with Honours, concentrating on Genetics and Evolution at the University of Calgary. I am a research assistant for the Cheng Lab at the University of Calgary's Foothills Campus, where I am investigating the effects of ERK inhibition on protein synthesis in Fragile X models using techniques such as SUnSET assay and FUNCAT. I am a Medical Office Assistant for Marlborough Medical Clinic. As well, I am the Vice President of Events for the Children's Cottage Ucalgary, where I organize events and festivals for vulnerable families in the Calgary community. I am currently pursing a career in the medical field of pediatrics or obstetrics and gynaecology.

Investigating the effects of selective inhibition of ERK signaling on protein synthesis in a mouse model of Fragile X Syndrome

Demi Ma[1,2,3], Seong Eon Ha[3], Dorit Moehrle[1,2,3], Ning Cheng[1,2,3]

[1]Faculty of Veterinary Medicine, University of Calgary; [2]Alberta Children's Hospital Research Institute, Cumming School of Medicine, University of Calgary; [3]Hotchkiss Brain Institute, Cumming School of Medicine, University of Calgary

UNIVERSITY OF CALGARY

Background

- **Fragile X Syndrome (FXS)** is caused by mutations in the Fragile X Messenger Ribonucleoprotein 1 (*FMR1*) gene, which leads to the loss of Fragile X Messenger Ribonucleoprotein (FMRP) resulting in secondary increase in protein synthesis[1].
- Common symptoms of FXS in humans: atypical social interactions, seizures, and heightened anxiety[1].
- Currently, there is no cure for FXS[1].
- The **extracellular signal-regulated kinase (ERK) pathway** is a signaling cascade that plays a key role in physiological processes[3].
  - ERK activation results in increased protein synthesis[3].
  - In humans and mouse models of FXS, ERK signaling is thought to be upregulated[3].
- **PD325901 (PD)** is a selective inhibitor of the ERK pathway, preventing the phosphorylation and activation of ERK[4].

Objective

- To determine if using PD can correct excessive brain protein synthesis in the *Fmr1* knockout (KO) mouse model.

Methodology

Surface Sensing of Translation (SUnSET):
Incorporates puromycin into growing polypeptide chains, allowing for quantification of protein synthesis rates.

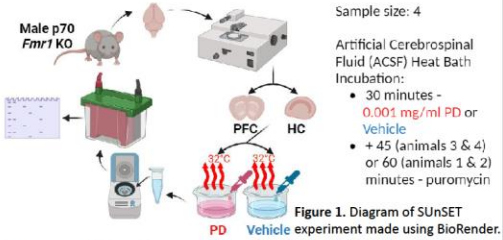

Figure 1. Diagram of SUnSET experiment made using BioRender.

Fluorescent Non-canonical Amino Acid Tagging (FUNCAT):
Provides good spatial resolution and investigation of specific regions and sub-populations of cells throughout the brain.

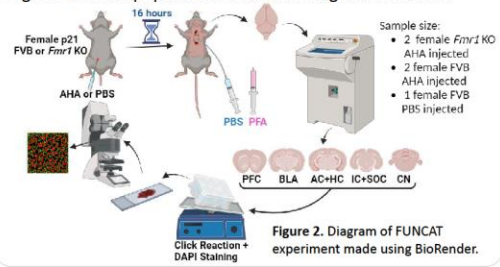

Figure 2. Diagram of FUNCAT experiment made using BioRender.

Summary

SUnSET:

- With ERK inhibition, protein synthesis can still occur; possibly due to other pathways.
- In the hippocampus (HC), there is a trend of decrease in puromycin signal and significant decrease in total ERK signalling in PD treated tissue.
  - This suggests that PD may decrease protein synthesis in the HC.
- In the prefrontal cortex (PFC), there is no direct correlation between protein synthesis and ERK inhibition.
- PD correction may have different effects across various brain regions.

FUNCAT:

- When comparing the animals injected with AHA versus PBS, there are more cells observed under the Cy3 staining in the AHA-injected animals.
- The increased Cy3 intensity in the *Fmr1* KO mouse compared to the FVB mice indicates an increase in protein synthesis.
- The Superior Olivary Complex (SOC) is typically very difficult to extract; therefore, FUNCAT allows us to study various brain regions that cannot be achieved through SUnSET.

Results

SUnSET

Antibody + Concentration	Hippocampus (HC)
β-Actin 1:1500	
ERK 1:2000	
phosphorylated ERK (pERK) 1:1000	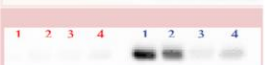
Puromycin 1:750	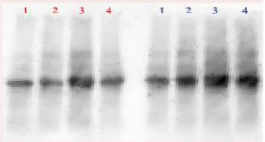

Figure 3. Western Blot images of the HC tissue. Mice 1 & 2 were incubated in puromycin for 60 minutes and mice 3 & 4 were incubated in puromycin for 45 minutes. Red represents PD treated tissue and blue represents vehicle treated tissue.

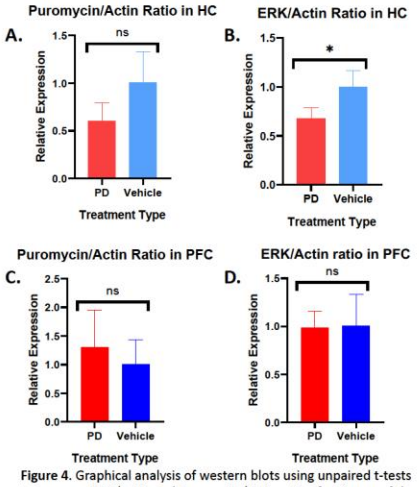

Figure 4. Graphical analysis of western blots using unpaired t-tests to compare ERK/Actin and Puromycin/Actin ratios for tissues of the prefrontal cortex (PFC) and HC. Significant p-value of p>0.05. **4A.** p=0.0828 **4B.** p=0.0246 **4C.** p=0.4677 **4D.** p=0.9852. Bars present standard error and "ns" represents non-significant values.

FUNCAT

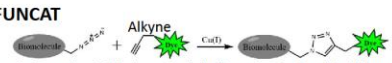

Figure 5. Example of click chemistry labelling using Cy-3 and Azidohomoalanine (AHA). Image taken from ABP Biosciences.

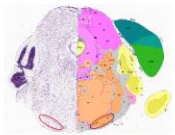

Figure 6. The red circle highlights the Superior Olivary Complex (SOC). Image taken from the Allen Reference Atlas.

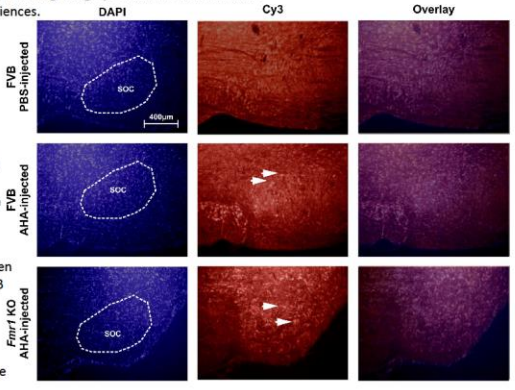

Figure 7. DAPI and Cy3 staining taken under a 10x microscope for the FVB PBS-injected, FVB AHA-injected, and *Fmr1* KO AHA-injected mice. DAPI depicts the cell nuclei, while Cy3 depicts newly synthesized peptides. The overlay depicts where the cells are localized.

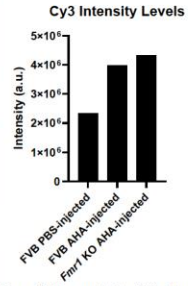

Figure 8. Bar graph depicting the Cy3 staining intensity levels between the FVB PBS-injected, FVB AHA-injected, and *Fmr1* KO AHA-injected mice.

Discussion

- Depending on the brain region using SUnSET, it is promising that PD may be able to correct excessive protein synthesis.
- Combining FUNCAT and specific biomarker staining, the determination of cell types and cell localization can be revealed. This allows us to narrow down the brain region of interest.

Future Directions

- Optimizing experimental conditions for both SUnSET and FUNCAT
- Larger sample size for both SUnSET and FUNCAT.
- Looking at sex differences in both FUNCAT and SUnSET.
- Examining the effects of PD in FUNCAT.

References

1. Bagni C, Tassone F, Neri G, Hagerman R. Fragile X syndrome: Causes, diagnosis, mechanisms, and therapeutics. American Society for Clinical Investigation; 2012 Dec 3; 22(12):4314-4322.
2. Hagerman RJ, Berry-Kravis E, Hazlett HC, Bailey DB, Moine H, Kooy RF, Tassone F, Gantois I, Sonenberg N, Mandel JL, Hagerman PJ. Fragile X syndrome. Nature reviews Disease primers. 2017 Sep 29;3(1):1-9.
3. Sawicka K, Pyronneau A, Chao M, Bennett MV, Zukin RS. Elevated ERK/p90 ribosomal S6 kinase activity underlies audiogenic seizure susceptibility in fragile X mice. Proceedings of the National Academy of Sciences. 2016 Oct 11;113(41):E6290-7.
4. The Pharmaceutical Company. Mirdametinib. 2022 Jun 4. https://nciformulary.cancer.gov/available_agents/Mirdametinib.htm

ALBERTA INNOVATES | HOTCHKISS BRAIN INSTITUTE | Owerko CENTRE | Alberta Children's HOSPITAL RESEARCH INSTITUTE | UNIVERSITY OF CALGARY FACULTY OF VETERINARY MEDICINE

The Effect of Prebiotic Fibre Supplementation on Macrophage Infiltration in Inguinal Adipose Tissue of Male Sprague Dawley Rats

Type of project: Summer
Supervisor(s): Dr. Walter Herzog

About the Researcher

Ayesha Rehan

Hi, I am Ayesha Rehan! I recently completed my 3rd year of my Biological Sciences degree and am preparing to pursue an Honours project in my upcoming final year. From the outset, biology captivated me by offering a window into the intricate workings of human systems and the fundamental components of life that shape our existence. My passion lies in preventative research, exploring ways in which we can proactively contribute to healthier lifestyles. An ambition for medicine, coupled with the practical application of scientific knowledge, deeply resonates with me as it bridges the gap between theory and making a tangible impact. Outside of the realm of science, I enjoy losing myself in a good book, traveling the world, or experimenting in the kitchen with new recipes, I value the balance these pursuits bring to my busy life as a university student. My research journey unfolded for me through a campus club, joining the lab was a turning point where I found genuine joy in conducting experiments and being an active participant in scientific discovery. However, navigating the vast expanse of preliminary research required before delving into my experiments proved a significant challenge. Reflecting on this experience, I realize the immense value in practically applying theoretical knowledge—a lesson I will carry forward into my future endeavors. For those embarking on a similar path, my advice is simple yet invaluable: ask questions relentlessly and supplement your learning with diligent research. This blend of curiosity and self-directed inquiry forms the cornerstone of successful research pursuits.

Effect of Prebiotic Fibre Supplementation on Macrophage Infiltration in Inguinal Adipose Tissue of male Sprague Dawley rats

Ayesha Rehan[1], Nada Abughazaleh[2,3,4], Ruth-Anne Seerattan[2], Walter Herzog[2,3,4]
[1]Biological Sciences, University of Calgary, [2]Human Performance Laboratory, Faculty of Kinesiology, University of Calgary, [3]Biomedical Engineering, University of Calgary, [4]McCaig Institute for Bone and Joint Health, University of Calgary

Introduction

Obesity, along with its associated low-level systemic inflammation, is linked to an elevated susceptibility of osteoarthritis (OA)[1]. Inflammation, stemming from adipose tissue (AT) expansion, and subsequent increased infiltration of macrophages has been linked to increased expression of proinflammatory cytokines[2]. Prebiotic fibre supplementation (PFS) has previously been shown to reduce this low-level chronic inflammation and mitigated knee joint OA when combined with a high-fat and high-sucrose (HFS) diet[3]. Our study focused on examining macrophage infiltration in Inguinal adipose tissue (IAT) in rats fed a HFS diet with fiber supplementation introduced at age 15 weeks. We hypothesized that the HFS diet will result in increased macrophage infiltration in IAT, and that the PFS will reduce macrophage infiltration when compared to the HFS group.

Methods

Twelve-week-old, male Sprague Dawley rats were randomized into three groups: control (chow diet, n=6), high-fat/high-sucrose diet introduced at age 12 weeks (HFS, n=6), and HFS diet with a PFS (HFS+F, n=6) introduced at age 15 weeks. Rats were sacrificed at age 24 weeks, and IAT was collected. Macrophages were labeled using CD68-specific antibodies, and DAPI (4'-6-diamidino-2-phenylindole) was applied to visualize nuclei. Crown-like structures (CLS), indicative of macrophage infiltration, were quantified manually and normalized to the cross-sectional area of the sample. Adipocyte cell size distribution in these rats was determined using image J.

Results

No significant differences in CLS were observed among HFS, HFS+F, and chow diet group rats. (Figure 1; $p>0.05$). Rats in the HFS group had more large cells (3000-6000 µm²) compared to Chow group rats ($p=0.00$) and fewer small cells (<500 µm²) than Chow group rats ($p=0.00$). Rats in the PFS diet group had significantly more small cells (<500 µm²) than the HFS diet group rats ($p=0.007$).

Conclusions

Consumption of a HFS diet for 12 weeks did not significantly affect macrophage infiltration into the IAT, despite a significant increase in the average adipocyte size in the HFS compared to the control group rats. PFS mitigated adipocyte expansion but had no measurable effect on macrophage infiltration.

References

[1]Hotamisligil (2017) Nature, 542:177.
[2]Jung et al. (2014) Int J Mol Sci, 15:6184.
[3] Rios et al. (2019) Sci Rep, 9:3893

Figures

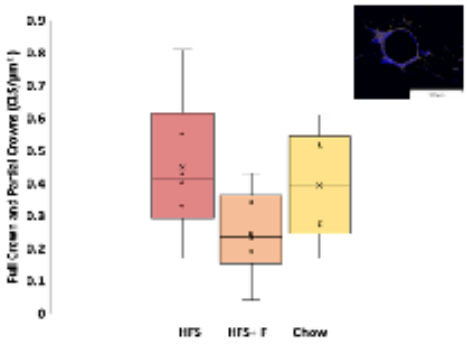

Figure 1. Number of crown-like structures in chow, HFS and HFS+F group rats (left). Image of a crown-like structure in which macrophages encircle an adipocyte (right).

The Effect of Prebiotic Fibre Supplementation on Macrophage Infiltration in Inguinal Adipose Tissue of Male Sprague Dawley Rats

Ayesha Rehan[1] Nada Abughazaleh[2,3,4], Ruth-Anne Seerattan[2], Walter Herzog[2,3,4]
[1]Biological Sciences, University of Calgary, [2]Human Performance Laboratory, Faculty of Kinesiology, University of Calgary, [3]Biomedical Engineering, University of Calgary, [4]McCaig Institute for Bone and Joint Health, University of Calgary

Background

- Obesity → Osteoarthritis (OA)[1]
- Weight bearing joints → OA caused by increased mechanical stress
- Non-weight bearing joints → OA linked to **low-level systemic inflammation**
- Adipocyte Expansion → Systemic Inflammation
  - Hypertrophy and Hyperplasia
  - Increased macrophage infiltration → Crown-like structures (CLS)[2]
- Prebiotic Fiber Supplementation (PFS) → mitigates obesity by reducing fat content and improving metabolic health[3]

Purpose: Investigate mechanisms of macrophage infiltration in the inguinal fat of male Sprague Dawley rats

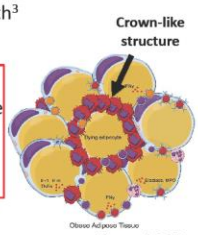

Khan et al, 2020

Methods

Twelve-week-old, male Sprague Dawley rats
- Control (chow, n=6)
- High-fat/high-sucrose (HFS, n=6)
- HFS with PFS (HFS+F/delayed, n=6).

Rats were sacrificed at twenty-four weeks.

Inguinal adipose tissue (IAT) was collected

Macrophages were labelled
- CD68-specific antibodies → macrophage
- DAPI (4'-6-diamidino-2-phenylindole) → nuclei

CLS were quantified
- Image J
  - Normalized to cross sectional area
- Kruskal-Wallis Testing

Results

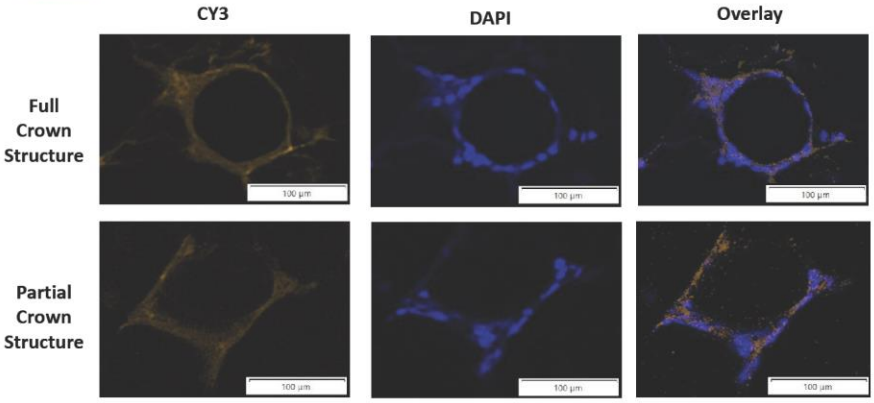

Images of crown-like structures are presented; full crowns encompass the entirety of the adipocyte, while partial crown-like formations encircle regions around the adipocyte but do not completely encompass

Figure 1. Graph showing the number of crown-like structures in three different experimental groups.

First Step → Adipocyte Expansion

- The HFS diet group had more larger cells compared to the Chow group ($p<0.05$)
- The PFS diet group had significantly more smaller cells than the HFS diet group ($p<0.05$)

Second Step → Macrophage Infiltration

- **No significant differences** in full crowns and partial crown-like structures in the HFS, HFS+F, and chow diet groups ($p>0.05$)

Discussion

- A trend of reduced CLS formation in the tissue of rats subjected to the PFS diet observed
- Potential cause of results → **Adipocyte location**
- IAT → situated beneath the skin in the lower body[4]
- In IAT, indirect release of metabolites into the portal system → **Reduced inflammation**[4]
- Visceral adipose tissue (VAT) → located within the abdominal cavity[4]
- VAT's proximity to internal organs enables direct influence on metabolic processes → Increased metabolic dysregulation[4]
- The absence of significant results in macrophage infiltration → potentially due to **IATs lower metabolic activity**

Conclusion:

- Consumption of a HFS diet for 12 weeks → No significant effect on macrophage infiltration into the IAT
- PFS →
  - Mitigated adipocyte expansion
  - No measurable effect on macrophage infiltration.

Future Directions

- Prolonging the study duration → enhance macrophage proliferation, as the formation of CLS takes more time compared to other degradation processes
- Altering the fat and sucrose content in the experimental design to observe potential influence

References

[1] Hotamisligil G. S. (2017). Nature, 542, 177–185

[2] Jung et al. (2014). Int J Mol Sci, 15(4), 6184–6223

[3] Rios et al. (2019). Sci Rep, 9(1):3893

[4] Chusyd et al. (2016). Front Nutr. 19;3:10

Ayesha Rehan
ayesha.rehan@ucalgary.ca